



# The direct and ocean-mediated influence of Asian orography on tropical precipitation and cyclones

Jane Wilson Baldwin<sup>1</sup> · Gabriel A. Vecchi<sup>2</sup> · Simona Bordoni<sup>3</sup>

Received: 8 June 2018 / Accepted: 4 January 2019 / Published online: 29 January 2019  
© Springer-Verlag GmbH Germany, part of Springer Nature 2019

## Abstract

Prior global climate model (GCM) experiments have shown that the Tibetan Plateau and related orography play a significant role in enhancing the Indian Monsoon, particularly during its onset, and the East Asian monsoon. However, these experiments have been largely performed with atmosphere-only, lower-resolution GCMs that neglect the influence of atmosphere–ocean coupling, and do not resolve tropical cyclones (TCs). Here we explore the influence of Asian orography on tropical circulations in a Geophysical Fluid Dynamics Laboratory GCM at two different atmosphere/land resolutions (~50 and 200 km), and with or without atmosphere–ocean coupling. Atmosphere–ocean coupling is found to play a significant role in the precipitation response due to the Asian orography, enhancing the precipitation increase over the Western North Pacific (hereafter WNP), and drying the Arabian Sea. In these same regions, the higher resolution model, which resolves TCs up to category 3, suggests that Asian orography has a significant influence on TCs, increasing TC frequency in the WNP, and decreasing it in the Arabian Sea. However, in contrast to precipitation, this TC response does not appear to be strongly affected by the atmosphere–ocean coupling. Connections between the direct atmospheric circulation response to Asian orography, ocean circulation changes, and these various effects on precipitation and tropical cyclones are analyzed and discussed.

**Keywords** Orography · Monsoon · Tropical cyclone · Asia · Atmosphere–ocean coupling

## 1 Introduction

Precipitation in South and East Asia is dominated by the seasonal monsoons, which are more dramatic than anywhere else on the planet. The South Asian Monsoon is characterized by high moist entropy over South Asia especially the Bay of Bengal, seasonally reversing winds over the Arabian Sea, and summer rainfall across South Asia (Molnar et al. 2010). The East Asian Monsoon is composed of strong spring and summer rainfall over East China and along a band across Korea and Japan and into the WNP (the Meiyu-Baiu) (Molnar et al. 2010). The rainfall of both these

summer monsoons is vital for agriculture—even small shifts in timing of the South Asian monsoon can be devastating for crop yields (Gadgil and Kumar 2006). The rainfall can also be a hazard causing dramatic flooding (Krishnamurthy et al. 2018). Despite these significant impacts, the mechanisms driving these climatic phenomena are still a topic of debate. Clarifying understanding of Asian monsoon dynamics is critically important for better prediction of monsoonal rainfall in the present climate, and preparation for how these systems might change under increased atmospheric concentration of carbon dioxide. Climate projections in the broad Asian monsoon region remain highly uncertain (Stocker 2014), highlighting our still limited understanding of monsoon dynamics and the need for progress.

General circulation models (GCMs) of the earth’s atmosphere are capable of simulating the Asian monsoons, albeit with varying degrees of skill (Boos and Hurley 2013). Thus, targeted experiments with GCMs can be used to disentangle the fundamental drivers of these monsoons. A suggested key factor for both the South and East Asian Monsoons is Asian orography. Including the Tibetan Plateau and Himalayas, these are the highest mountains on earth and stretch

✉ Jane Wilson Baldwin  
janewb@princeton.edu

<sup>1</sup> Princeton Environmental Institute, Princeton University, Guyot Hall, Princeton, NJ 08544-1003, USA

<sup>2</sup> Department of Geosciences, Princeton University, Guyot Hall, Princeton, NJ 08544, USA

<sup>3</sup> Environmental Science and Engineering, California Institute of Technology, Mail Code 131-24, Pasadena, CA 91125-2300, USA

over a vast territory (Fig. 1a). Experiments removing the Tibetan Plateau and related orography (compared to control simulations with full orography) were performed with some of the earliest GCMs by Hahn and Manabe (1975). They used an atmosphere-only GCM with prescribed SSTs and a resolution of about 270 km, and simulated less than a year focused on the summer months. Despite the relatively crude GCM and short simulation, they reached a number of conclusions that remain robust today. In particular, they found the Tibetan Plateau is associated with middle and upper atmosphere heating and high pressure, upward motion and low surface pressure over India, and northward extension of the South Asian monsoon rainfall.

Since this pioneering study, numerous groups have adopted similar GCM experiment designs to further understand the related monsoon dynamics and other climatic influences of these mountains. Precipitation changes typical of many of these studies are summarized in Fig. 2, which shows results from simulations with and without Asian orography from the atmosphere-only 200 km resolution GCM GFDL-AM2.1. The mountains clearly enhance the South Asian Monsoon (e.g., Prell and Kutzbach 1992; Abe et al. 2003), though whether this influence is primarily mechanical or thermal remains a topic of significant debate (Ye and Wu 1998; Wu et al. 2012; Boos and Kuang 2010, 2013). Asian orography also dries extratropical Asia, and is fundamental to the existence of deserts such as the Gobi and Taklimakan (Broccoli and Manabe 1997; Abe et al. 2005; Baldwin and Vecchi 2016). They also enhance the East Asian Monsoon, especially the Meiyu-Baiu, and are likely

more essential to its existence than to the South Asian Monsoon (Chen and Bordoni 2014; Molnar et al. 2010; Tang et al. 2012; Sampe and Xie 2010; Lee et al. 2015). The heating of the middle atmosphere by monsoonal latent heat release, which is amplified by the mountains, can drive remote drying over the Mediterranean and the North African and Southwest Asian dry zones (Rodwell and Hoskins 1996; Simpson et al. 2015). The Tibetan Plateau is also found to shape the storm track over Asia in a variety of ways, including driving the midwinter suppression of the Pacific storm track activity (Lee et al. 2013). Some of these studies have explored the impact of smaller portions of the Asian mountain system both to refine understanding and to simulate paleoclimatic periods (Tang et al. 2012; Baldwin and Vecchi 2016; Shi et al. 2014, 2008). These studies suggest that location can be just as important for climatic influence as size of mountains. For example, simulations indicate that the Mongolian Plateau, which lies north of the Tibetan Plateau, plays a bigger role in the atmospheric stationary wave pattern than the Tibetan Plateau, despite its smaller size (White et al. 2017). Despite these significant advances, there are still a number of aspects of the climatic influence of Asian orography that remain uncertain. Topics of debate this work seeks to address include details of seasonality of response, the role of atmosphere–ocean coupling, and influence of model resolution and extreme events.

Many prior studies of topographic response have focused on one season, for example JJA to capture most of the Asian monsoon. Going beyond total monsoon response to examine monsoon seasonality, Park et al. (2012) found

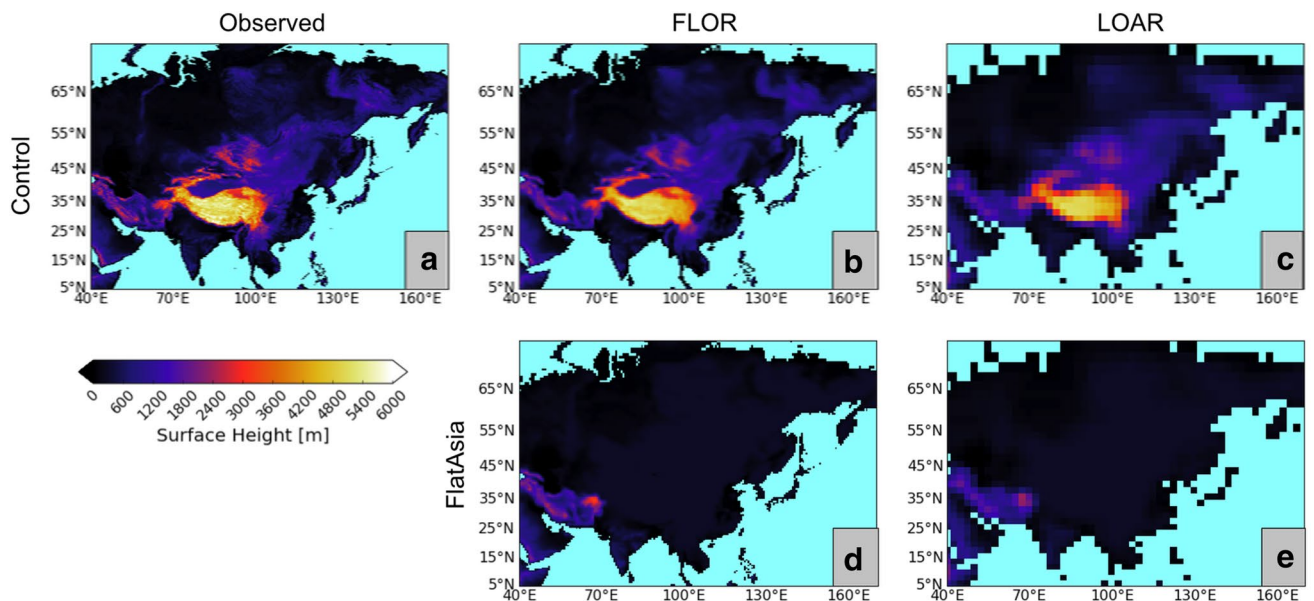


**Fig. 1** Topographic boundary conditions for the GCM simulations. Surface height is shown for the Control (**a–c**) and FlatAsia (**d, e**) experiments. Observed 5' resolution modern day topography (**a**;

Edwards 1988) is presented for comparison to FLOR (**b**) and LOAR (**c**) boundary conditions

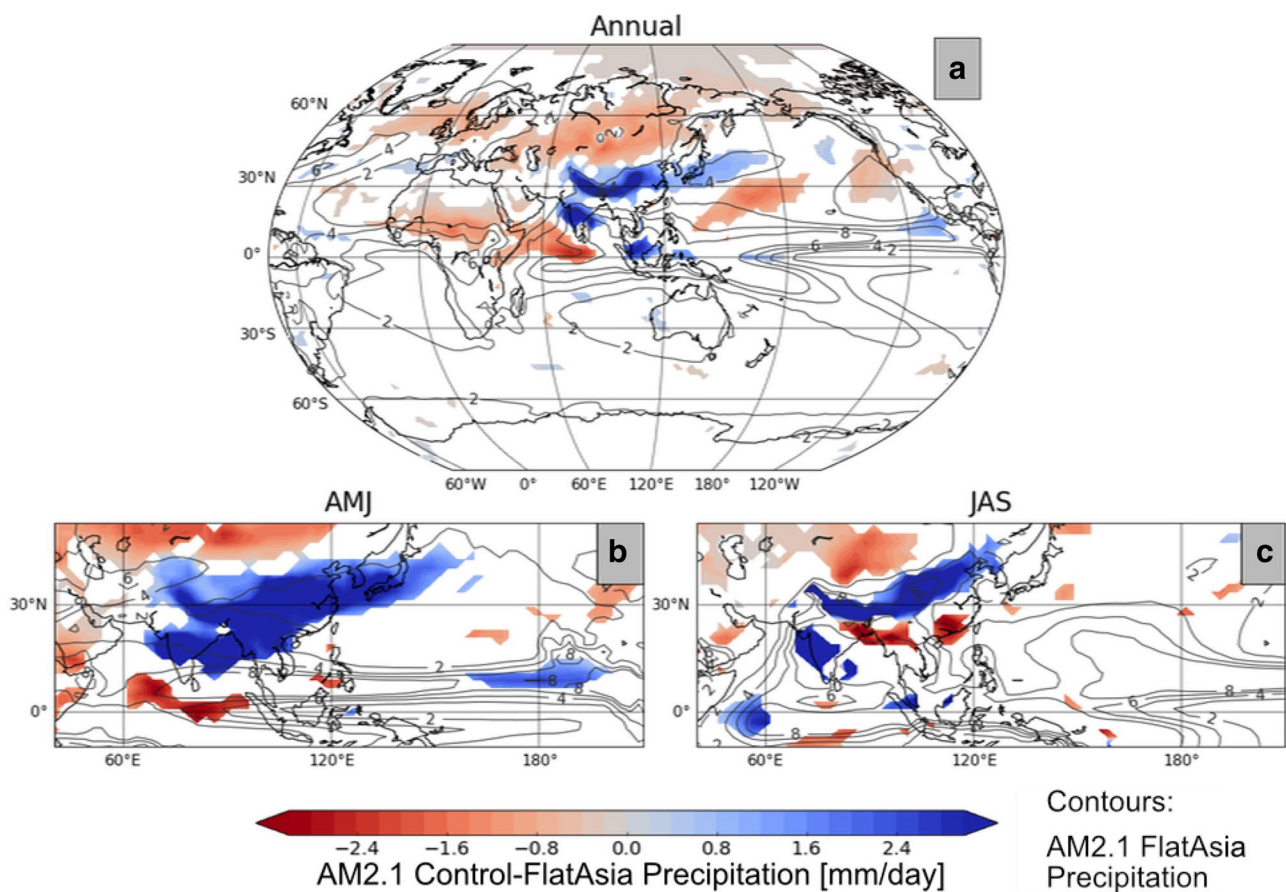


**Fig. 2** Influence of Asian orography on precipitation in an atmosphere-only model (AM2.1). Change in precipitation (AGCM Control–AGCM FlatAsia) is shaded and AGCM FlatAsia mean precipitation is contoured globally for the annual mean (**a**), and over the WNP

and northern Indian Ocean for AMJ (**b**), and JAS (**c**). Anomalies are only shown where statistically significant at the 95% level based on a two-sided *t* test. See Table 2 for details on the GCM simulations used in this study

that the Tibetan Plateau significantly increases WNP precipitation during the monsoon onset period (AMJ), but only very weakly increases it during the monsoon peak (JAS). To explain this effect, they invoke mechanical influences of the southern Tibetan Plateau on the westerly jet which drive downstream convergence and precipitation in a moist atmosphere, consistent with arguments by Takahashi and Battisti as reported by Molnar et al. (2010). Another recent paper found that the Meiyu-Baiu's convection, which dominates summer precipitation in the WNP, is driven primarily by meridional dry enthalpy advection associated with the Tibetan Plateau's stationary wave pattern (Chen and Bordoni 2014). The influence over the WNP appears large and somewhat nonintuitive in seasonality, meriting further exploration.

In addition to limits in the seasonality explored, original studies examining the influence of Asian orography were performed with atmosphere-only GCMs with prescribed SSTs (e.g., Hahn and Manabe 1975). Due to lack of atmosphere–ocean coupling, such experiments do not capture

the role of air-sea interaction in influencing monsoon precipitation. This is problematic given significant interaction between the monsoon winds and ocean current changes documented in prior work (e.g., Leetmaa 1972). In light of this, a number of studies have performed topographic flattening experiments incorporating air–sea interaction. These studies include global atmosphere models coupled to slab ocean models (Prell and Kutzbach 1992; Kutzbach et al. 1993; Kitoh 1997; Park et al. 2012), global atmosphere models coupled to more fully resolved oceans (Rind et al. 1997; Kitoh 2002; Abe et al. 2004, 2013; Kitoh 2004; Abe et al. 2005; Kitoh 2007; Kitoh et al. 2010; Abe et al. 2013; Lee et al. 2013, 2015; He et al. 2018), one study with full atmosphere–ocean coupling over only the tropics (Okajima and Xie 2007), a GCM model of intermediate complexity (Koseki et al. 2008), and a high-resolution regional climate model coupled to a mixed-layer ocean model (Wang et al. 2018). Different levels of coupling are often examined in these studies via AGCMs or nudged SST experiments. While details differ, these studies typically

indicate that atmosphere–ocean coupling enhances the precipitation response to Asian orography, and can alter the monsoon onset times of various basins. Asian orography exerts a strong influence on SSTs in the WNP, with warming between about  $0^{\circ}$  and  $20^{\circ}\text{N}$  and cooling between about  $20^{\circ}$  and  $50^{\circ}\text{N}$ , with the low-latitude SST warming enhancing monsoonal precipitation. Asian orography also consistently cools the Arabian Sea. Despite the general consistency in the pattern of SST changes, questions remain regarding the mechanisms of the SST change, particularly the role of ocean transport versus changes to surface energy balance.

Regarding model resolution, most prior studies exploring the influence of Asian orography employ a typical GCM atmospheric and land resolution of about  $2^{\circ}/200\text{ km}$ . As noted in prior studies, there is a need to examine topographic influence in higher resolution models (Kitoh et al. 2010; Lee et al. 2015). Higher resolution atmosphere/land has a few advantages in studying precipitation around Asia. First, it captures with greater fidelity than lower resolution models the height of tall mountains critical for the monsoon circulation such as the Himalayas and lower mountains that shape local patterns of precipitation (Boos and Kuang 2010; Kapnick et al. 2014; Baldwin and Vecchi 2016). This leads to improved simulation of the Asian monsoons (Delworth et al. 2012). Second, sufficiently high resolution atmospheres permit formation of TCs, or typhoons as they are called around Asia, which are responsible for significant seasonal and extreme rainfall (Khouakhi et al. 2016). While relatively high resolution regional climate models and atmosphere-only GCMs (AGCMs) have been used to study the climatic impacts of Asian orography (Kitoh et al. 2010; Ma et al. 2014; Wang et al. 2018), there is as yet no investigation of the influences of Asian orography using a high resolution atmosphere–ocean coupled GCM (AOGCM).

In this study we further explore the role of mountains in Asian summer monsoon precipitation by using a state-of-the-art high resolution AOGCM. GFDL CM2.5-FLOR, the GCM employed, has an approximately  $50\text{ km}$  resolution atmosphere model coupled to a  $1^{\circ}$  fully resolved ocean model. We flatten topography across Asia, with the largest modification where topography is highest and broadest (i.e., the Himalayas and Tibetan Plateau). While other studies have examined the influence of Asian mountains on winter storms (Park et al. 2010; Lee et al. 2013), to our knowledge this is the first set of simulations able to examine how TCs are influenced by Asian orography. We also performed additional experiments to isolate the role of high resolution and atmosphere–ocean coupling in our results. Regarding TCs, we employ a GCM called LOAR identical to FLOR except with a lower atmospheric and land resolution ( $\sim 200\text{ km}$ ), which limits TC formation. Regarding SST changes, we run simulations of both FLOR and LOAR with SSTs nudged such that the mountain removal cannot influence SSTs

except at very short timescales. This set-up is advantageous over simply prescribing SSTs as it allows high frequency air-sea interaction important for realistic simulation of TCs, and tropical rainfall and its variability (Barsugli and Battisti 1998). The SST nudging process also produces metrics which allow us to distinguish the role of ocean transport versus changes in surface energy balance in the mountain-caused SST changes. Altogether, our study contributes new investigation of atmosphere–ocean coupling in Asian orographic influence, exploration of more details of seasonality of response especially over the WNP, and for the first time examination of the role of these mountains in shaping the climatology of TCs.

Section 2 describes the GCMs used in this study in more detail, the observations employed for model validation, and the analysis strategy. Section 3 provides results, describing changes in precipitation, SSTs, and TCs induced by the Asian mountains. Finally, Sect. 4 summarizes the results and provides discussion and conclusions.

## 2 Methods

### 2.1 Models

We utilize two Geophysical Fluid Dynamics Laboratory (GFDL) fully coupled atmosphere–ocean GCMs in this study. FLOR (Vecchi et al. 2014; Jia et al. 2014), which is the Forecast-oriented Low Ocean Resolution derivative of CM2.5 (Delworth et al. 2012), has a relatively high resolution  $\sim 50\text{ km}$  atmosphere and land, and a relatively lower resolution  $\sim 1^{\circ}$  ocean. LOAR is identical to FLOR in every regard except for its atmosphere and land resolution, which is a more standard GCM resolution of  $\sim 200\text{ km}$ . The high resolution of FLOR allows it to simulate TCs up to Category 3 in strength, while LOAR does not simulate such circulation extremes. Additionally, FLOR resolves high and sharp topographic features, such as the Himalayas, more accurately than LOAR (Fig. 1). All simulations employ the LM3 land model, run with static, modern-day vegetation (Milly et al. 2014).

This family of models’ simulation of a variety of climatic phenomena has been examined and validated. Most relevant to the present work are prior studies utilizing these models’ simulation of Asian precipitation (Baldwin and Vecchi 2016), extreme precipitation (van der Wiel et al. 2016), and global and WNP TCs (Vecchi et al. 2014; Krishnamurthy et al. 2016; Zhang et al. 2016). GFDL CM2.5, which has the same atmosphere as FLOR, exhibits a much improved simulation of monsoon precipitation compared to GFDL CM2.1, which is similar to LOAR (see Fig. 7 in Delworth et al. (2012)).

To gain perspective on these GCMs' simulation accuracy, we also use Coupled Model Intercomparison Project Phase 5 (CMIP5) pre-industrial control run data from 30 different GCMs (Taylor et al. 2012). The CMIP5 models utilized and their modeling centers are listed in Table 1.

## 2.2 Observational datasets

To validate the models' simulation of precipitation, we employ three observed precipitation datasets (TRMM, CMAP, and GPCP). TRMM stands for the "Tropical Rainfall Measuring Mission" and is a multisatellite-based precipitation product covering 50°S–50°N across the globe and available at a 0.25° resolution (Huffman et al.

2007); data from January 2000 to September 2010 is used in this study. CMAP is a merger of five different satellite products spanning the entire globe (Xie and Arkin 1997), while GPCP is a merger of both satellite and ground-based observations (Adler et al. 2003). Both are available at a 2.5° resolution, and data from 1979–2012 are used. To validate the GCMs' simulation of winds, we utilize monthly wind data from the MERRA reanalysis (Rienecker et al. 2011).

Additionally, for some nudged SST model experiments (Nudged2Obs; see Table 2) we employ a climatology derived from the Met Office Hadley Centre SST data (Rayner et al. 2003). AM2.1 is forced with a climatology derived from years 1950–1998 of the Reynolds reconstructed SST dataset (Reynolds et al. 2002).

**Table 1** CMIP5 GCMs used for validation of the FLOR and LOAR simulations, and the modeling centers that created each GCM. We use monthly precipitation data from each GCM's pre-industrial control run

GCM	Modeling center
ACCESS1-0	Commonwealth Scientific and Industrial Research Organization and Bureau of Meteorology
BCC-CSM1.1	Beijing Climate Center
BNU-ESM	College of Global Change and Earth System Science, Beijing Normal University
CanESM2	Canadian Centre for Climate Modelling and Analysis
CCSM4	National Center for Atmospheric Research
CMCC-CM	Euro-Mediterraneo sui Cambiamenti Climatici
CNRM-CM5	Centre National de Recherches Meteorologiques / Centre Europeen de Recherche et Formation Avancees en Calcul Scientifique
CSIRO-Mk3.6.0	Commonwealth Scientific and Industrial Research Organization in collaboration with Queensland Climate Change Centre of Excellence
FGOALS-g2	LASG, Institute of Atmospheric Physics, Chinese Academy of Sciences; and CESS, Tsinghua University
FGOALS-s2	LASG, Institute of Atmospheric Physics, Chinese Academy of Sciences
GFDL-CM3	NOAA Geophysical Fluid Dynamics Laboratory
GFDL-ESM2G	
GFDL-ESM2M	
GISS-E2-H	NASA Goddard Institute for Space Studies
HadGEM2-CC	Met Office Hadley Centre
HadGEM2-ES	
INM-CM4	Institute for Numerical Mathematics
IPSL-CM5A-LR	Institut Pierre-Simon Laplace
IPSL-CM5A-MR	
IPSL-CM5B-LR	
MIROC-ESM	Atmosphere and Ocean Research Institute (The University of Tokyo), National Institute for Environmental Studies, and Japan Agency for Marine-Earth Science and Technology
MIROC-ESM-CHEM	
MIROC4h	
MIROC5	
MPI-ESM-LR	Max Planck Institute for Meteorology
MPI-ESM-MR	
MPI-ESM-P	
MRI-CGCM3	Meteorological Research Institute
NorESM1-M	Norwegian Climate Centre
NorESM1-ME	

**Table 2** GCM simulations employed in this study

Experiment name	Topography	Radiative forcing year	SSTs	GCMs used
AGCM Control	Modern	1991–2000	Forced with observed climatology	AM2.1
Fully Coupled Control		1860	Freely evolving	LOAR, FLOR
Nudged2Model Control			Restored to Control climatology	
Nudged2Obs Control			Restored to observed climatology	LOAR
AGCM FlatAsia	Asia flat	1991–2000	Forced with observed climatology	AM2.1
Fully Coupled FlatAsia		1860	Freely evolving	LOAR, FLOR
Nudged2Model FlatAsia			Restored to Control climatology	
Nudged2Obs FlatAsia			Restored to observed climatology	LOAR

## 2.3 Experiments

For both FLOR and LOAR, experiments are run with two different topographic boundary conditions, which will be referred to as “Control” and “FlatAsia”. In Control, present-day topography is used as a boundary condition for the model. In FlatAsia, topography over most of Asia is flattened to the elevation of the surrounding landscape (300 m), with the most dramatic changes around the Tibetan Plateau and Himalaya where the present-day elevation is greatest (Fig. 1). This alteration is performed in boundary conditions controlling surface height, gravity wave drag, and boundary layer roughness as in Baldwin and Vecchi (2016). Initializing FlatAsia simulations with extant atmospheric initial conditions adjusted to Control orography causes model instabilities. As a result, all experiments are run from a “cold” start, without atmospheric initial conditions, which allows the model to more robustly adjust to the presence or absence of Asian topography.

We perform an additional set of experiments to isolate the direct climatic influence of Asian orography from that mediated through changing SST. In these experiments (the “nudged SST” versions of both Control and FlatAsia) SSTs are restored to repeating monthly climatologies (Murakami et al. 2015; Zhang et al. 2015). We nudge to each model’s respective monthly climatology calculated from 100 years of Control run data using a 5-day restoring timescale, effectively removing the influence of flattening Asian topography on climatological SSTs in the FlatAsia experiment. In LOAR, we also ran a set of experiments nudged to the observed SST climatology from HADISST; in addition to removing low frequency atmosphere–ocean coupling, these experiments also eliminate model biases in SST. Importantly, SST nudging still allows high frequency air-sea interaction important for TCs and tropical precipitation. This experimental set-up with nudging to both model and observed SSTs is similar to that used in He et al. (2018), except with nudging rather than AGCM simulations.

Table 2 provides a summary of all the GCM simulations examined for this study, other than the CMIP5 simulations used for model validation.

## 2.4 Analysis strategy

The FLOR Fully Coupled Control experiment was run for 1000 years, and the FLOR Fully Coupled FlatAsia experiment was run for 100 years. Unless otherwise noted, we analyze years 31–100 of both to allow for some model spin-up. LOAR Fully Coupled experiments are run for 300 years each, since the low resolution makes this a more efficient and faster model to run, and we analyze years 201–300. FLOR and LOAR nudged SST experiments are initialized from year 101 of their associated Fully Coupled simulation. FLOR nudged SST experiments are run for 30 years (through year 130) and all 30 years are analyzed. LOAR nudged SST experiments are run for 200 years (through year 300) and years 201–300 are analyzed.

Prior work has suggested that the Tibetan Plateau exerts a significant influence on deep ocean circulation, in particular decreasing the Atlantic Meridional Overturning Circulation (AMOC) (Fallah et al. 2015). Due to the long timescales associated with these circulations, the ocean in the Fully Coupled FlatAsia simulations may not stabilize from the Fully Coupled Control state it is initialized from for thousands of years. Due to computational limitations, we only run our simulations for hundreds of years, so the continued deep ocean adjustment will be ongoing over the period of analysis. However, we do not expect this to significantly bias results over the regions of interest for this study (i.e., the WNP and Arabian Sea).

Model-generated TCs are tracked using an algorithm developed by Harris et al. (2016). The algorithm primarily depends on 6-hourly instantaneous sea-level pressure, 10-m winds, 850 mb relative vorticity, and atmospheric temperature anomalies between 300 and 500 mb. TC track density is determined by counting TC positions for each  $1^\circ \times 1^\circ$  grid box, then smoothing this count using a 9-point moving

average weighted by distance from the center of the grid box. These values are then integrated annually, so TC density results are presented in units of number of TCs per year.

Many result figures will be presented as Control minus FlatAsia (Control – FlatAsia), which can be imagined as the climatic effect of uplifting Asian orography. Statistical significance of most such results is determined using a two-sided *t* test evaluated at a 95% level. The percent of change in a given quantity due to SST change induced by Asian mountains (i.e., the role of atmosphere–ocean coupling) can be quantified as:  $((\text{Control} - \text{FlatAsia}) - (\text{Nudged2Model Control} - \text{Nudged2Model FlatAsia})) / (\text{Control} - \text{FlatAsia}) \times 100$ .

### 3 Results

#### 3.1 Model validation

We test the accuracy of LOAR and FLOR's simulation by comparing to observed and reanalyzed wind and precipitation data. The comparison is imperfect for a number of reasons, including the shorter temporal span of the observations, and that the LOAR and FLOR simulations have pre-industrial 1860 radiative forcings while the observations

are from the late 20th to early 21st century. Nonetheless, the model validation provides important perspective for interpreting the experimental results.

Overall, LOAR and FLOR both provide a reasonably accurate simulation of the large-scale features of summer precipitation and wind across Asia, but exhibit a few notable biases compared to observations (Fig. 3). Both GCMs underestimate the strength of the Findlater Jet over the Arabian Sea in AMJ, and exhibit northerly winds over the western side of the basin less present in observations. Rainfall over the Western Ghats on the west coast of India is also weaker in the GCM than observations. FLOR tends to have improved performance compared to LOAR in simulating the spatial distribution of precipitation over places with complex topography, such as the Himalayas (Fig. 3). However, both models appear to have a low bias in precipitation over the Bay of Bengal. Over the southern WNP, precipitation is biased a bit high in LOAR and a bit low in FLOR, straddling the observations.

FLOR and LOAR both capture the general seasonal cycle of precipitation seen in the observations over the southern WNP (Fig. 4). Precipitation peaks in August in both LOAR/FLOR and observations, but in LOAR/FLOR reaches a minimum one month later in March rather than February. Both models' precipitation falls within the range of observations

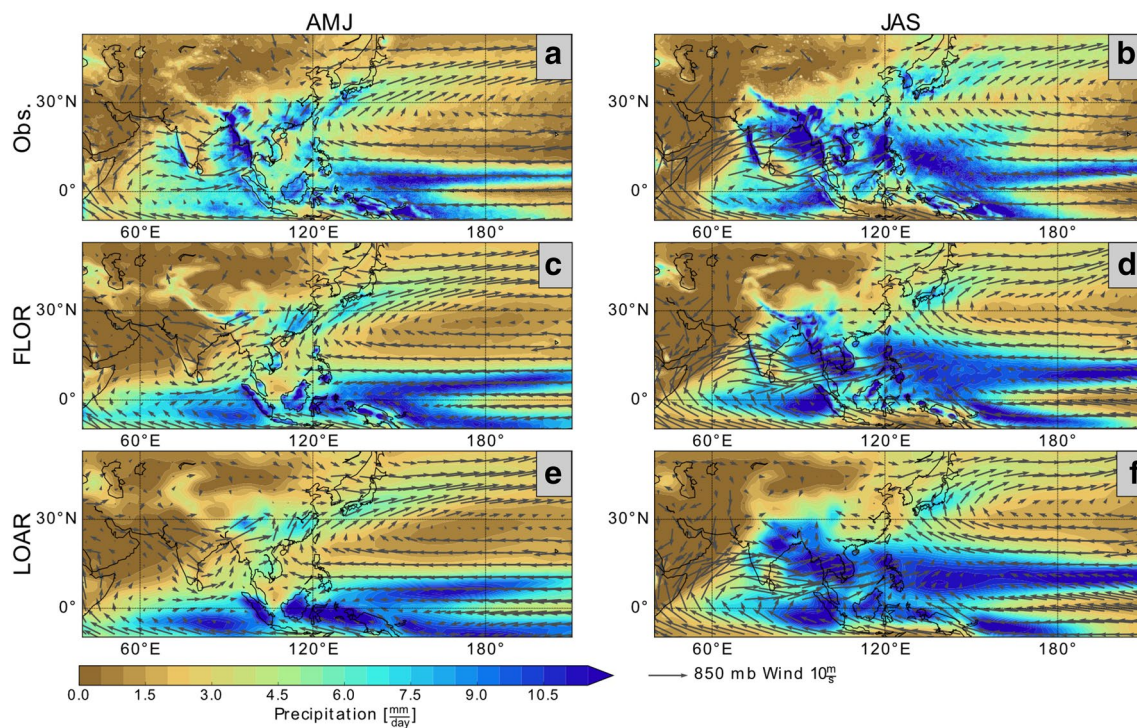
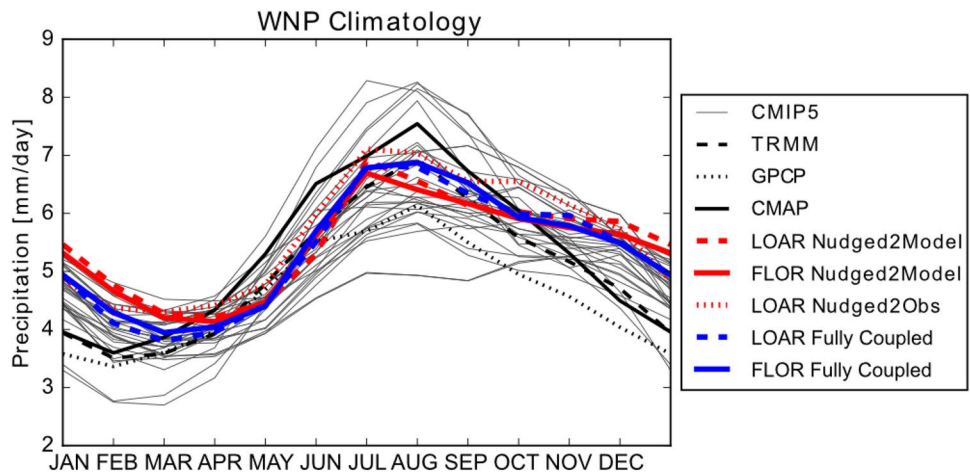


**Fig. 3** Precipitation and winds in observations, FLOR, and LOAR. Precipitation and 850 mb wind are shown over the Asian sector for observations (**a, b**), FLOR Fully Coupled Control (**c, d**), and LOAR Fully Coupled Control (**e, f**) for the monsoon onset period AMJ (**a, c**,

**e**) and the monsoon peak period JAS (**b, d, f**). Observed precipitation data is from TRMM, and observed wind data is from the MERRA reanalysis

**Fig. 4** Seasonal cycle of WNP precipitation in FLOR/LOAR compared to observations and other models. Precipitation averaged over  $0^{\circ}$ – $40^{\circ}$  N and  $110^{\circ}$ – $180^{\circ}$  W is plotted for TRMM, GPCP, and CMAP observed data (black), CMIP5 models (grey), and LOAR and FLOR Fully Coupled (blue) and SST nudged simulations (red). For all the FLOR and LOAR data, simulations with Control topography are used



in the summer, but exhibits high biases in the winter typical of CMIP5 models. The LOAR Nudged2Obs simulation also exhibits this bias, albeit somewhat less so than the FLOR and LOAR Nudged2Model experiments. This suggests that SST biases in the Fully Coupled simulations may contribute to the winter precipitation biases, but do not fully explain them.

Keeping these various strengths and biases of the GCMs in mind, we proceed with examination of precipitation, SST, and TC changes due to Asian orography.

### 3.2 Precipitation

In the annual mean, Asian orography generally enhances precipitation over the Asian monsoon sectors and the WNP, but dries extratropical Asia and farther west into the Mediterranean and Sahel (Fig. 5). These large-scale changes are similar to what is found with lower-resolution, atmosphere-only models (Fig. 2). The precipitation response also appears to be quite similar between FLOR and LOAR. This is interesting because in FLOR Asian orography forces large changes in TCs not simulated in LOAR due to its low resolution (Fig. 6, discussed in detail in Sect. 3.4). This suggests that the presence or absence of TCs does not significantly affect the large-scale precipitation pattern, which seems consistent with observational estimates suggesting TCs only contribute 25% or less of rainfall over the WNP in the present climate (Khouakhi et al. 2016; Jiang and Zipser 2010). In the following results, where data from only one of FLOR or LOAR is shown the results are qualitatively the same and quantitatively similar for both.

On a seasonal basis, key differences compared to prior studies emerge. Unlike Park et al. (2012), Asian orography increases WNP precipitation throughout the entire summer monsoon season, including the onset (AMJ) and peak (JAS) (Fig. 7). In AM2.1, the AMJ precipitation increase is focused around  $30^{\circ}$  N. In contrast, in LOAR (Fig. 7a) and

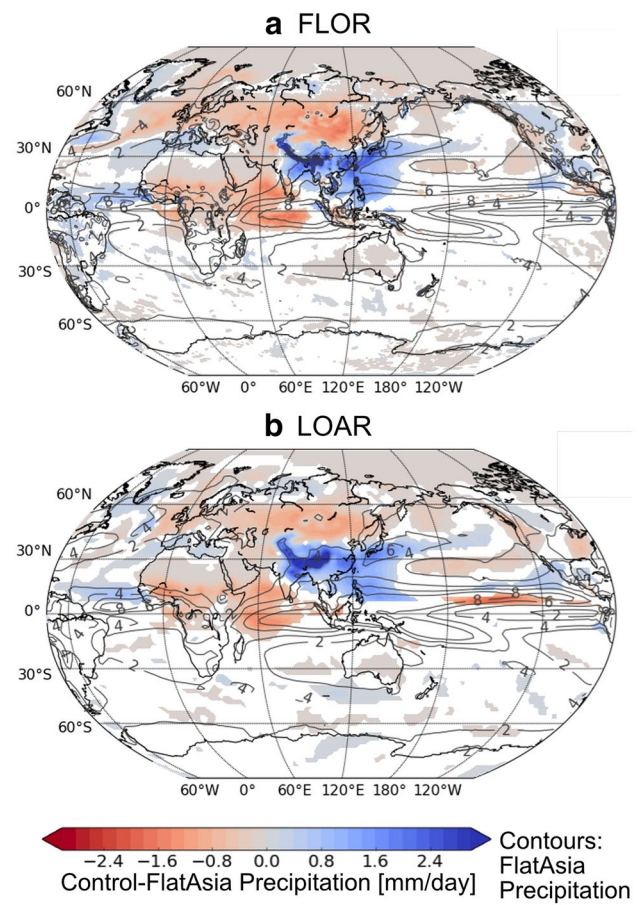
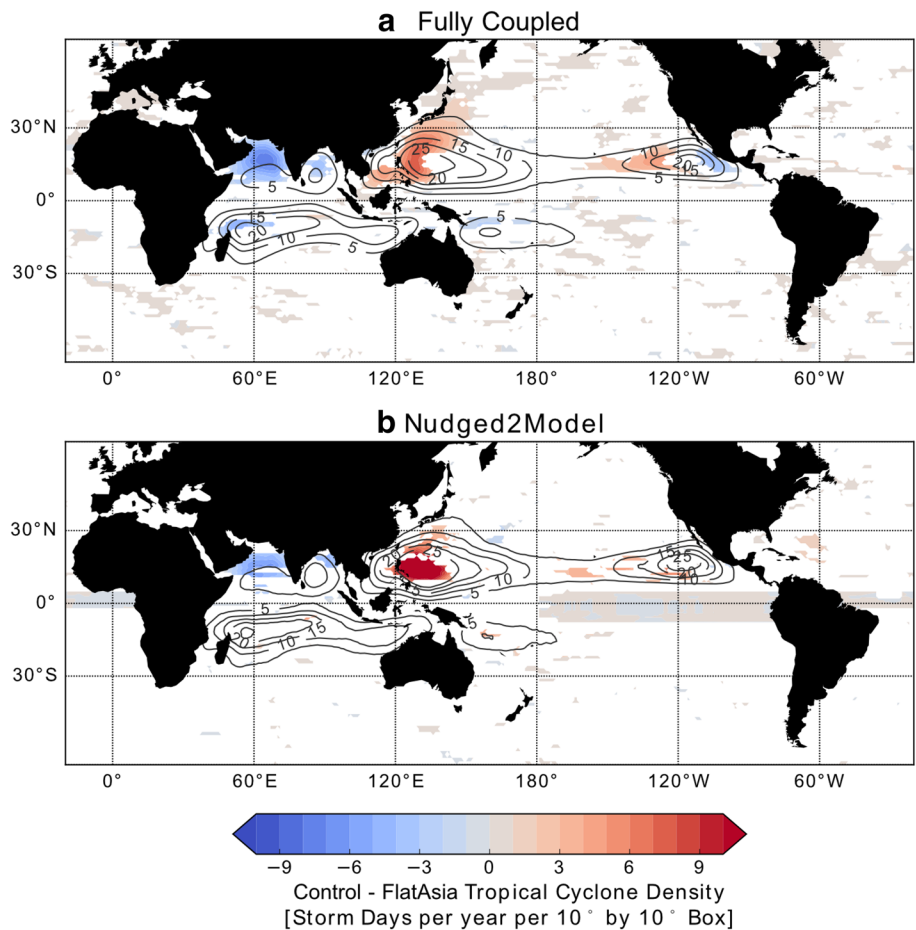


**Fig. 5** Annual mean precipitation changes induced by the Asian mountains. Annual mean change in precipitation (Fully Coupled Control – Fully Coupled FlatAsia) is shaded and Fully Coupled FlatAsia mean precipitation is contoured for FLOR (a) and LOAR (b). Anomalies are only shown where statistically significant at the 95% level based on a two-sided  $t$  test

**Fig. 6** TC density changes induced by Asian orography. FLOR TC changes due to Asian orography are shaded, and Control TC density is contoured for the Fully Coupled runs (**a**) and Nudged2Model runs (**b**). For this analysis only, all available years (1000 total) of the Fully Coupled Control simulation are used, with years 1–30 still thrown out to allow for model spin-up. Anomalies are only shown where statistically significant at the 90% level based on a two-sided *t* test. Note that the FLOR Nudged2Model simulations have only 30 years, which contributes to making those results less statistically significant



FLOR (not shown) the AMJ precipitation increase extends farther southward to about 10°N. The area-average AMJ precipitation increase also is approximately doubled in LOAR/FLOR compared to AM2.1 to a precipitation increase of about 20% (Fig. 8). As discussed in Sect. 1, atmosphere-only models including AM2.1 indicate that Asian orography does not enhance WNP precipitation during the monsoon peak. However, LOAR and FLOR exhibit significant increases in WNP precipitation during this season (Fig. 7b). Asian orography forces an increase in precipitation centered over Japan, and another one centered around 15°N, which extends far into the Pacific. The area-average precipitation increase induced by Asian orography is not as large as in AMJ in both absolute and percent terms (< 10%), however the anomaly importantly goes from zero or even negative to positive.

There are also strong Arabian Sea decreases in precipitation during the monsoon season not present in the AGCM simulations (Fig. 2 versus 7). Decreases of more than 2 mm/day occur in places where mean precipitation is not much more than that. Additionally, the drying appears to extend over Southern India. The precipitation decreases are stronger during the monsoon peak (JAS) than the monsoon onset (AMJ), suggesting an inverse link to monsoon circulations.

It is natural to ask the reasons behind these seasonal differences: are these due to the increased spatial resolution in FLOR or to air-sea coupling missing in previous studies? Because these WNP and Arabian Sea changes are found in both FLOR and LOAR, we conclude that increased spatial resolution and resulting TCs are not driving the differences in precipitation response between this study and prior studies. However, allowing the presence or absence of Asian orography to influence SSTs (via atmosphere-ocean coupling) does drive much of these differences. The enhancement of southern WNP precipitation and Arabian Sea drying are both more than doubled in many places due to atmosphere-ocean coupling (Figs. 7b, d and 8). In contrast, the northern WNP precipitation increase in JAS found in our simulations but not in Park et al. (2012) is not due to coupling. This change likely results from model differences not examined in this work, or possibly differences in where topography was flattened.

While not the focus of this work, the WNP winter precipitation changes tell an interesting and contrasting story to the summer results. Significant precipitation increases in the winter are found in the Fully Coupled and Nudged2Model runs, but not in the Nudged2Obs or AGCM runs (Fig. 8).

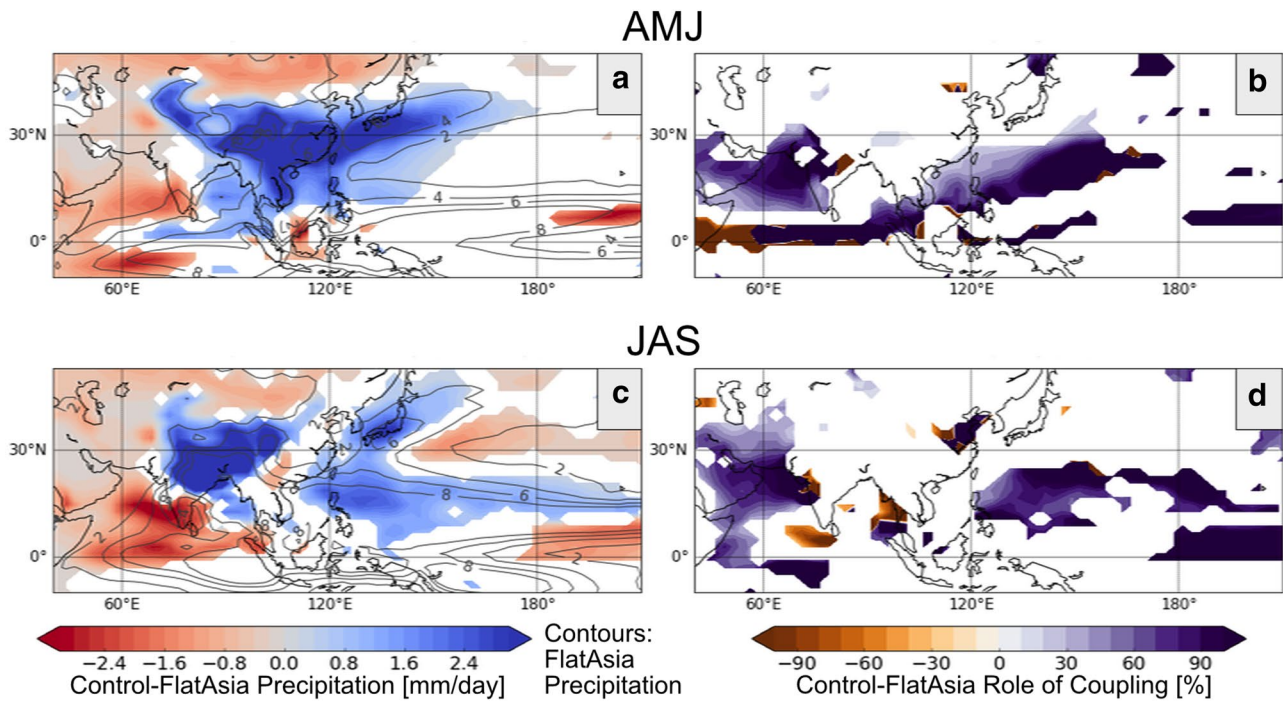


**Fig. 7** Seasonal precipitation changes induced by the Asian mountains and role of atmosphere–ocean coupling. Change in precipitation (Fully Coupled Control - Fully Coupled FlatAsia) is shaded and FlatAsia mean precipitation is contoured for LOAR AMJ (a) and JAS mean (b). The percent of precipitation change due to SST changes

induced by the Asian mountains is shaded for AMJ (a) and JAS (b) by comparing the Fully Coupled and Nudged2Model LOAR simulations (see Sect. 2 for description of this metric). Anomalies are only shown where statistically significant at the 95% level based on a two-sided *t* test

This suggests that the winter precipitation increase may be the result of model SST biases and is spurious. This is distinctly different from the summer precipitation change, in which the AGCM, Nudged2Model, and Nudged2Obs results are consistently less than the Fully Coupled results, and so atmosphere–ocean coupling clearly enhances the precipitation increase due to Asian mountains. LOAR SST biases exist throughout the year, but it appears they play a bigger role in skewing the precipitation change in winter.

### 3.3 Sea surface temperature (SST)

Asian orography drives strong SST changes in the WNP and Arabian Sea responsible for much of the precipitation change in these regions (Fig. 9). The WNP mostly warms between 0° and 30° N and cools from 30° to 60° N, as found in prior work (Kutzbach et al. 1993; Rind et al. 1997; Kitoh 1997, 2002; Okajima and Xie 2007). The Arabian Sea generally cools, which has also been highlighted in prior studies (Prell and Kutzbach 1992; Abe et al. 2004, 2013; Kitoh et al. 2010; Abe et al. 2013; Wang et al. 2018; He et al. 2018). These changes are consistent with enhanced precipitation in the southern WNP and drying of the Arabian Sea, as positive(negative) SST anomalies decrease(increase) static stability, and so increase(decrease) convection.

While the pattern of SST changes is consistent between many prior studies, there is disagreement regarding the role of surface energy balance versus ocean circulation in driving the changes. To clarify these mechanisms, we perform a decomposition of causes of SST change utilizing metrics from our SST nudging process. The GCM outputs metrics that can be used to quantify how much of the SST difference from the target SST is due to the energy transfer with the atmosphere versus ocean transport. The equation that governs SST in a nudged simulation can be summarized as follows:

$$\frac{\delta SST}{\delta t} = ADV + MIX + HFLUX + \frac{1}{\tau}(SST^* - SST), \quad (1)$$

where *ADV* and *MIX* represent fluxes from the ocean to the surface through advection and diffusion/mixing, respectively, *HFLUX* represents net heat fluxes between the atmosphere and the ocean surface (comprising longwave and shortwave radiation, and latent and sensible heat fluxes),  $\tau$  represents the relaxation timescale for the nudging (5 days in our simulations), and *SST\** represents the target SST being nudged to (in this study, Fully Coupled Control simulation climatology or observed climatology), and *SST* represents the model's SST. *HFLUX* and  $\frac{1}{\tau}(SST^* - SST)$  are diagnostics output by the model. These can be used to determine the energy

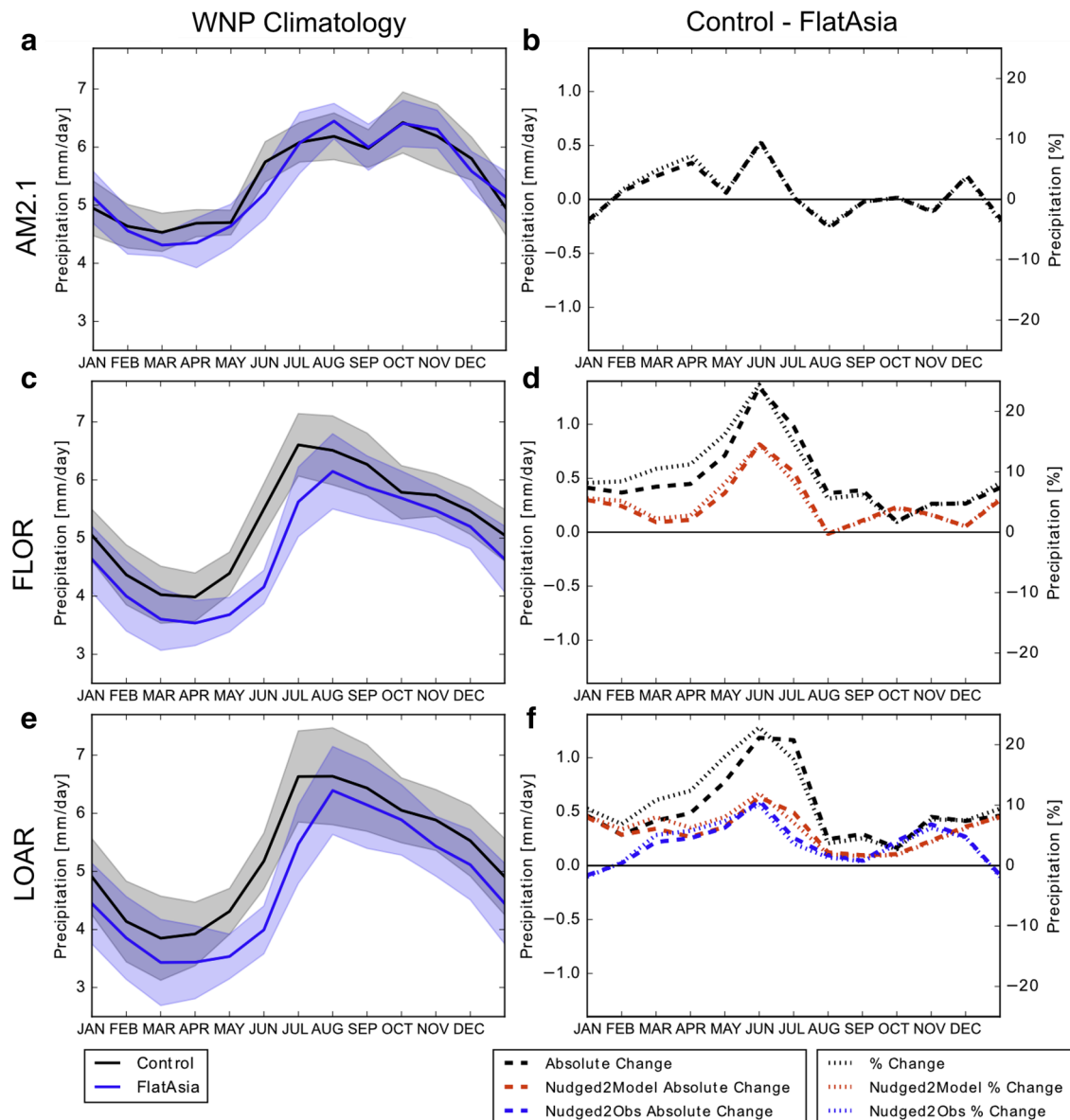


**Fig. 8** WNP precipitation climatology changes due to Asian orography for different GCMs. Results for the AGCM AM2.1 (**a, b**), FLOR Fully Coupled (**c, d**), and LOAR Fully Coupled (**e, f**) are compared. **a, c, e** Precipitation climatology is averaged over the WNP ( $0^{\circ}$ – $40^{\circ}$  N,  $110^{\circ}$ – $180^{\circ}$  W) and plotted for Control (black) and FlatAsia (blue) runs, with one standard deviation above and below shaded. **b, d, f**

Absolute (thick dash) and percent (thin dash) differences between Control and FlatAsia climatologies are plotted, showing results for the standard settings for each model in black (atmosphere-only for AM2.1, Fully Coupled for FLOR and LOAR), in red for Nudged2Model simulations, and in blue for Nudged2Obs simulations, where those simulations are available

transfer from ocean transport as follows. Assuming SST is in steady state so  $\frac{\delta SST}{\delta t} = 0$ , and grouping the terms associated with heat fluxes from the ocean ( $OCEAN = ADV + MIX$ ), Eq. (1) can be rearranged to:

$$OCEAN = -HFLUX - \frac{1}{\tau}(SST^* - SST). \quad (2)$$

In our simulations, comparing  $HFLUX$  and  $OCEAN$  indicates that the dipole of SST change in the WNP is due to

energy transfer with the atmosphere, while the Arabian Sea cooling is primarily due to ocean circulation changes (Fig. 10).

To further examine the WNP SST changes, we decompose the fluxes of energy between the atmosphere and ocean surface (Fig. 11). The Nudged2Model simulation data is used because it shows the initial atmospheric forcing on the ocean surface from Asian orography that drives the SST changes—the Fully Coupled simulation data is equilibrated

**Fig. 9** SST changes induced by the Asian mountains. Shaded are annual mean Control - FlatAsia differences in SST from LOAR Fully Coupled simulations, with LOAR Fully Coupled FlatAsia SST contoured. Anomalies are only shown where statistically significant at the 95% level based on a two-sided  $t$  test. The blue and red dashed shapes demarcate the WNP regions of cooling and warming averaged over for Fig. 11

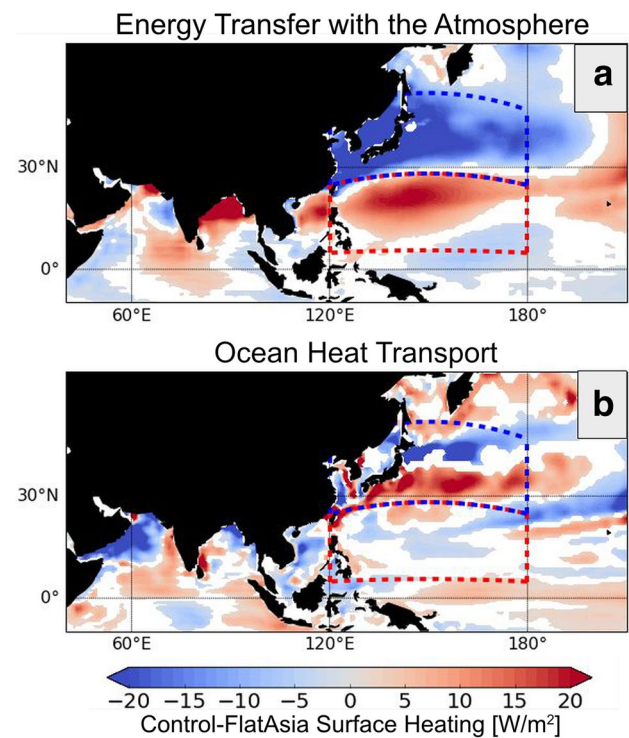
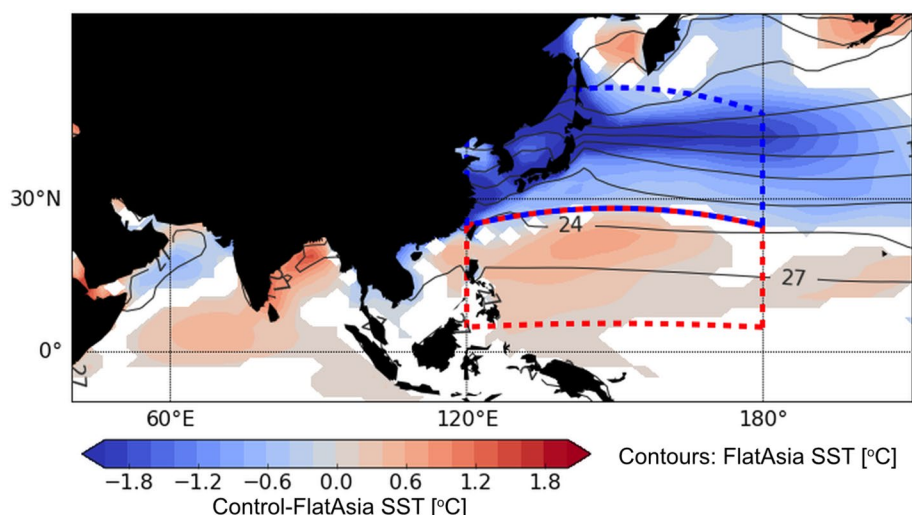


**Fig. 10** Oceanic versus atmospheric drivers of SST change. Shaded is Control - FlatAsia change in energy transfer from the atmosphere to the surface (*HFLUX*; **a**) and change in ocean heat transport (*OCEAN*; **b**). Data is from LOAR Nudged2Model simulations, and these metrics are calculated as part of the SST nudging in the GCM. Anomalies are only shown where statistically significant at the 95% level based on a two-sided  $t$  test

with the surface already and so is less informative. In the south, the warming is driven primarily by decreased latent heat fluxes. In the north, the cooling is driven by increased sensible heat fluxes, decreased shortwave radiation reaching the surface from cloud changes, and a smaller contribution

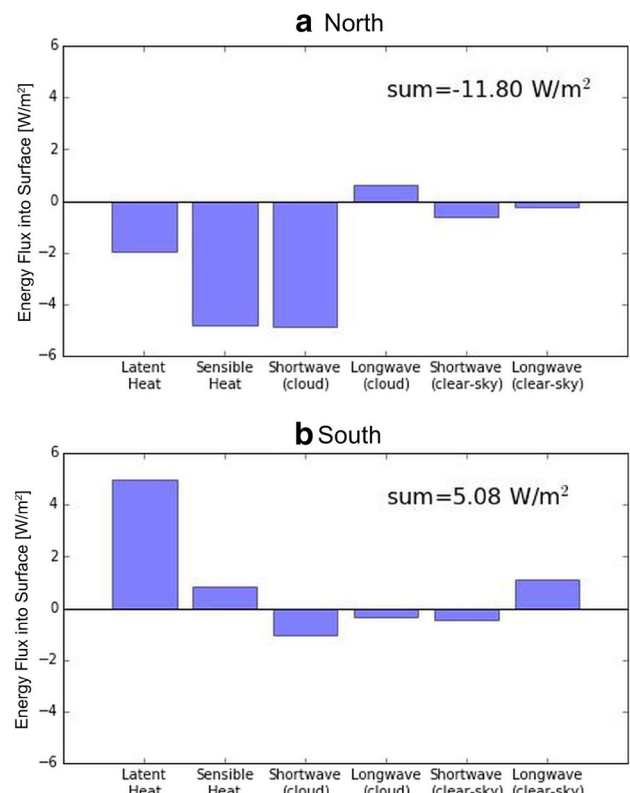


**Fig. 11** WNP surface energy balance changes. Control - FlatAsia change in different components of the surface energy balance is calculated from LOAR Nudged2Model simulations. Averages are calculated over the northern blue box (**a**) and southern red box (**b**) shown in Fig. 9. Positive values indicate greater energy going into the surface and warming (i.e., increase in latent/sensible heat fluxes out of the surface is a negative value)

from increased latent heat fluxes. Across the northern WNP region, increases in cloud cover occur at all levels, but most coherently at low and mid-levels (not shown).

In the south, decreased latent heat fluxes occur due to decreased wind speed. Asian orography generates a stationary wave (Hoskins and Karoly 1981), which includes a high-low-high geopotential height pattern emanating in a south-eastward direction from the Tibetan Plateau (Fig. 12). The first low and second high intersect around 120°–180° W and 15°–30° N depending on the pressure level, generating southwesterlies in this region. For all seasons other than JAS, there are mean easterlies in this region, thus the southwesterlies decrease wind speed and turbulent fluxes. The SST warming lags the wind speed changes such that warming is present throughout the year, as described in Okajima and Xie (2007). Thus, even though wind speed is not lessened over JAS, SSTs are still warmer and precipitation is increased.

In the north, the energy balance changes are driven by Asian orography enhancing the East Asian Winter and Summer Monsoons (Chiang et al. 2015; Liu and Yin

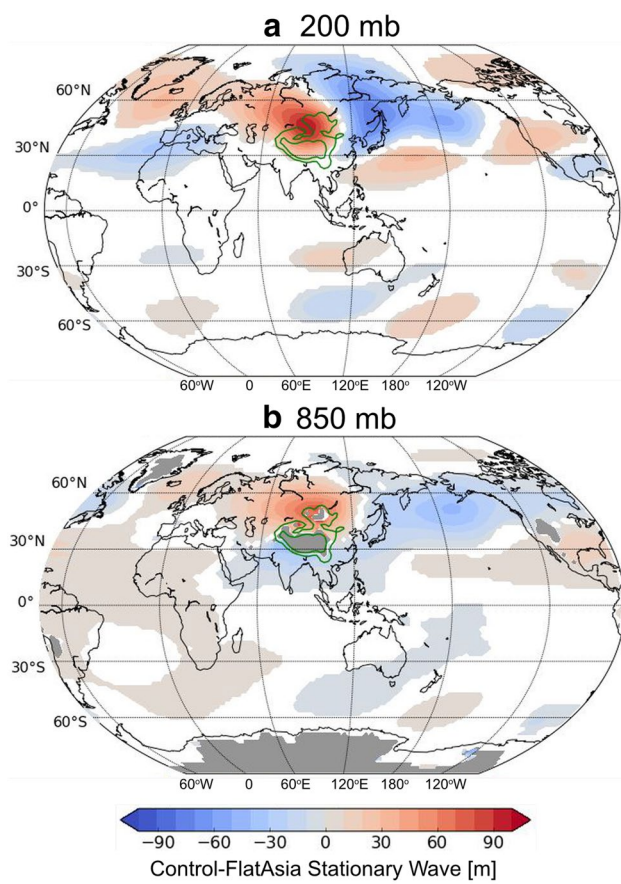


**Fig. 12** Stationary wave pattern induced by the Asian mountains. Annual mean Fully Coupled Control - FlatAsia differences in geopotential height with the zonal mean removed at 200 mb (**a**) and 850 mb (**b**). Green contours designate the region of topographic modification and grey shading shows where Control topography is higher than the relevant pressure level. Anomalies are only shown where statistically significant at the 95% level based on a two-sided  $t$  test

2002). In the winter, the enhanced Tibetan high (Fig. 12) generates northerly wind anomalies in northeastern Asia (Fig. 13; Lee et al. (2013)). These northerlies advect cold, polar air southward, where it is carried along the mean westerlies across the northern WNP. The increased surface-air temperature gradient increases both sensible and latent heat fluxes, cooling the northern WNP. Latent heat fluxes increase less than sensible because this region is cold, and because there are some compensating humidity increases. The cooling is stronger at low levels in the atmosphere (not shown), which increases static stability. In the northern WNP, increasing static stability increases low and mid-level stratus clouds, a result that has also been shown in other observational and modeling studies (Klein and Hartmann 1993; Norris and Leovy 1994; Clement et al. 2009). These clouds further exaggerate the initial cooling by decreasing shortwave radiation reaching the surface. In the summer months, prior studies demonstrate that the Tibetan Plateau leads to warm air advection across this region, fueling convection of the Meiyu-Baiu. Two mechanisms for this warm air advection have been proposed: (1) the enhanced Tibetan high leads the westerly jet to advect higher temperatures across China and Japan into the West Pacific (Sampe and Xie 2010), and (2) the Tibetan Plateau's stationary wave pattern generates southerlies in the WNP which advect warm air into the Meiyu-Baiu region (Chen and Bordoni 2014). Moist static energy budget analysis of AM2.1 simulations indicates that the latter mechanism is the primary driver (Chen and Bordoni 2014). Either way, the clouds associated with the Meiyu-Baiu further cool the northern WNP by reflecting shortwave radiation. In summary, Asian orography cools the northern WNP throughout the year, but via different mechanisms depending on the season.

The Arabian Sea SST cooling again is not driven through surface energy balance changes, but rather through ocean circulation changes. By blocking cool, dry extratropical air, the Himalayas increase moist entropy in South Asia and the Bay of Bengal, leading to off-equatorial maxima (Boos and Kuang 2010). This drives a longitudinally localized cross-equatorial overturning circulation (Hoskins and Wang 2006; Bordoni and Schneider 2008). At low-levels, northward flow in the northern hemisphere needs to be balanced by friction on westerly winds. Thus, the orography enhances summer low-level southwesterlies across the Arabian Sea known as the Findlater jet (Fig. 13), an effect shown in prior work such as Hahn and Manabe (1975). The associated southwesterly wind stresses along the land-sea boundary of Oman and Somalia induce coastal upwelling (Fig. 14). The upwelling of deeper, cold water cools the Arabian Sea surface, and reduces local precipitation.

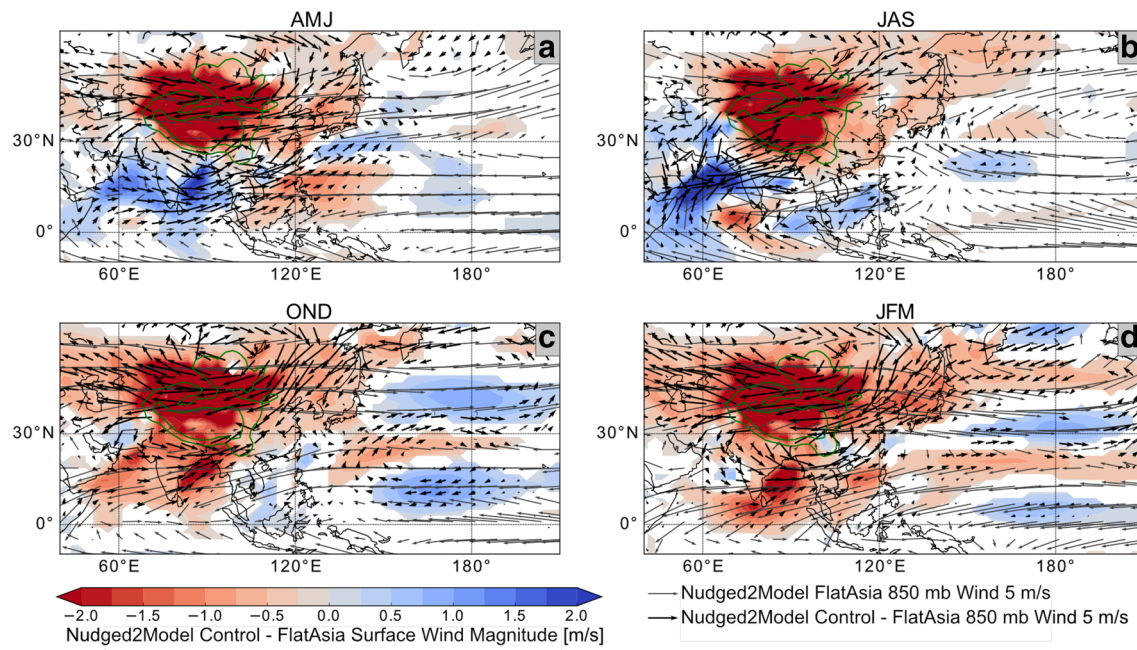
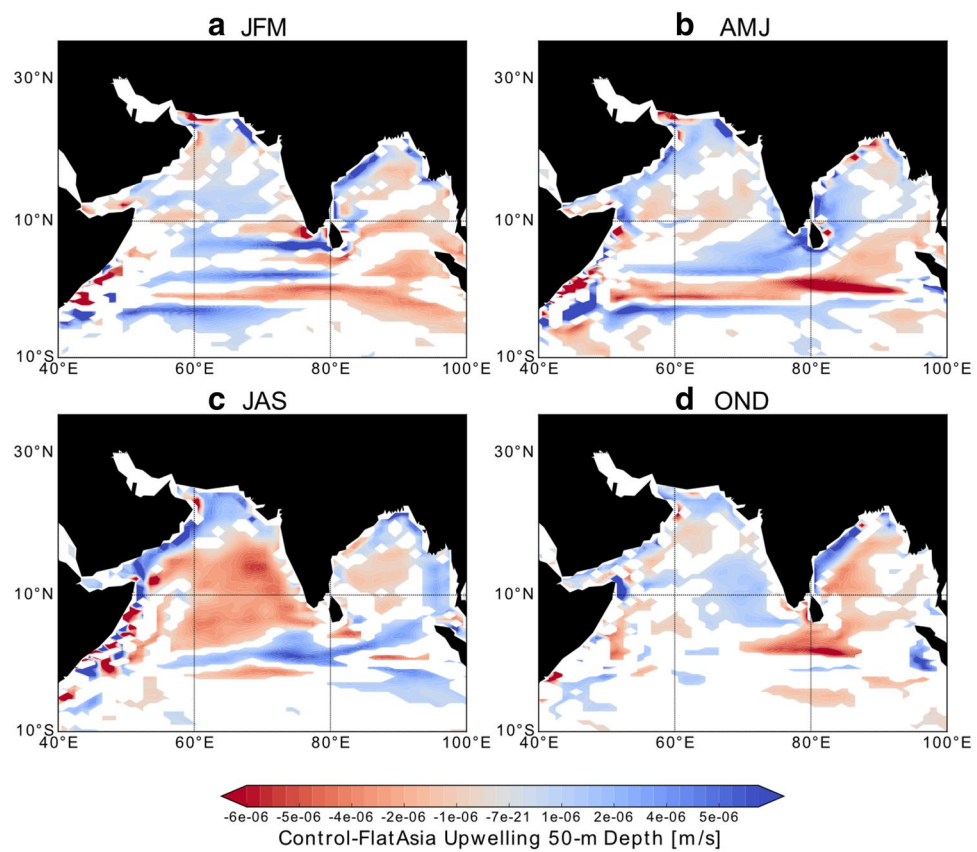


**Fig. 13** Seasonal changes in winds and wind speed induced by Asian mountains. Shaded Nudged2Model Control - FlatAsia differences in surface wind magnitude; Nudged2Model FlatAsia and Nudged2Model Control - FlatAsia 850 mb wind vectors are plotted in grey and black, respectively. Seasonal averages for AMJ, JAS, OND, and JFM are shown in panels **a–d**, respectively. Green contours designate

the region of topographic modification. Anomalies are only shown where statistically significant at the 95% level based on a two-sided *t* test. Nudged2Model simulation data is used to highlight that these changes are directly driven by atmospheric circulation changes without SST response to the orography. However, results from the Fully Coupled runs are largely similar

**Fig. 14** Seasonal 50-m depth ocean upwelling changes induced by the Asian mountains. Fully Coupled LOAR change in upwelling is shown for JFM (**a**), AMJ (**b**), JAS (**c**), and OND (**d**) seasonal means. Anomalies are only shown where statistically significant at the 95% level based on a two-sided *t* test



### 3.4 Tropical cyclones (TCs)

While found to be unimportant for the precipitation changes, the TC response to Asian orography is interesting in and of itself. It is also unexplored in prior work due to lack of TC-permitting GCMs. Asian orography yields a dramatic increase in TC density in the southern portion of the WNP, reaching 60% of the mean TC density (Fig. 6a). In contrast, in the Arabian Sea, Asian orography strongly suppresses the development of TCs. In the present very few TCs form in the Arabian Sea; it appears that this is largely due to the presence of Asian orography.

TC density change in a given location can occur due to alteration of TC genesis or tracks. A metric of TC genesis change also output by the TC tracker (not shown) exhibits a very similar spatial pattern of changes to the total TC density change, with decrease in the Arabian Sea, increase in the WNP, and some increase in the East Pacific. This suggests that the TC density changes due to Asian orography can largely be understood as the result of changes in TC genesis.

To examine the climatological drivers of the genesis change, we calculate a genesis potential (GP) index developed by Kerry Emanuel and used in Camargo et al. (2007):

$$GP = |10^5 \eta|^{3/2} \left( \frac{H}{50} \right)^3 \left( \frac{V_{pot}}{70} \right)^3 (1 + 0.1 V_{shear})^{-2}, \quad (3)$$

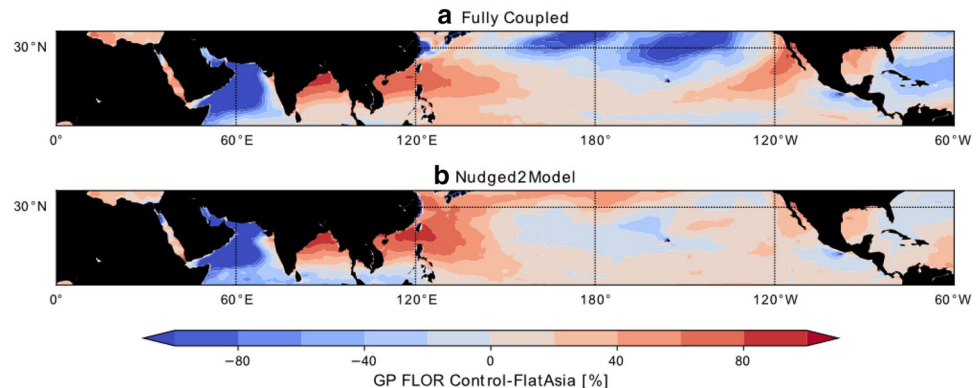
where  $\eta$  is the absolute vorticity at 850 mb,  $H$  is the relative humidity at 600 mb in percent,  $V_{pot}$  is the potential intensity (in  $\frac{m}{s}$ ), and  $V_{shear}$  is the magnitude of the vertical wind shear between 850 and 200 mb (in  $\frac{m}{s}$ ). High values of GP reflect climatic conditions favorable for TC genesis. Control - FlatAsia GP change exhibits a similar spatial pattern to the TC density and genesis changes, highlighting the relevance of this metric (Fig. 15a). We examine percent changes in the components of TC genesis to further disentangle the mechanisms through which Asian orography influences TC density (Fig. 16). All the components other than vorticity exhibit spatial patterns of change largely similar to the TC density

changes. 600 mb relative humidity and potential intensity exhibit the greatest magnitude of change, implying that these components drive the TC density changes.

We employ the Nudged2Model simulations to further probe the TC changes. In these runs the pattern and magnitude of TC density change is quite similar to the Fully Coupled runs (Fig. 6b), despite the fact that there are very limited SST changes and so potential intensity changes are smaller (Fig. 16). Due to the similarity between the Nudged2Model and Fully Coupled TC changes, we conclude that Asian orography's influence on SST is not critical to the TC change in these locations. Differences in relative humidity appear to be the primary cause of TC increase in the WNP and decrease in the Arabian Sea. In contrast, in the Eastern North Pacific there is a smaller increase in TC density that appears to be dependent on atmosphere–ocean coupling; we leave further exploration of the change in the East Pacific to future work.

Different circulation features drive the local relative humidity changes in the WNP and Arabian Sea. In the WNP, the intersection of the Asian mountains' stationary wave first low and second high drive southwesterlies (Fig. 17), and upward motion (not shown; Cohen and Boos 2017). Acting on the vertical and meridional moisture gradients, both of these flows increase relative humidity. In the Arabian Sea, the Asian monsoon's diabatic heating creates low pressure and cyclonic circulation, in accord with Gill (1980). This advects in dry air from the arid north and west (i.e., the Sahara and Mediterranean), which decreases relative humidity (Fig. 17). An additional contributing factor is the drying subsidence over the Kyzylkum desert north of the Arabian Sea, which is a remote response to the monsoon heating (Rodwell and Hoskins 1996). Asian orography suppresses TC activity in the Arabian Sea from May through November (not shown), spanning most times of year when TCs occur occasionally over this region in the present climate (Evan and Camargo 2011).

**Fig. 15** TC GP changes due to Asian orography. Results are shown for Control - FlatAsia with FLOR Fully Coupled (**a**) and Nudged2Model runs (**b**). % changes are calculated as (Control - FlatAsia)/Control



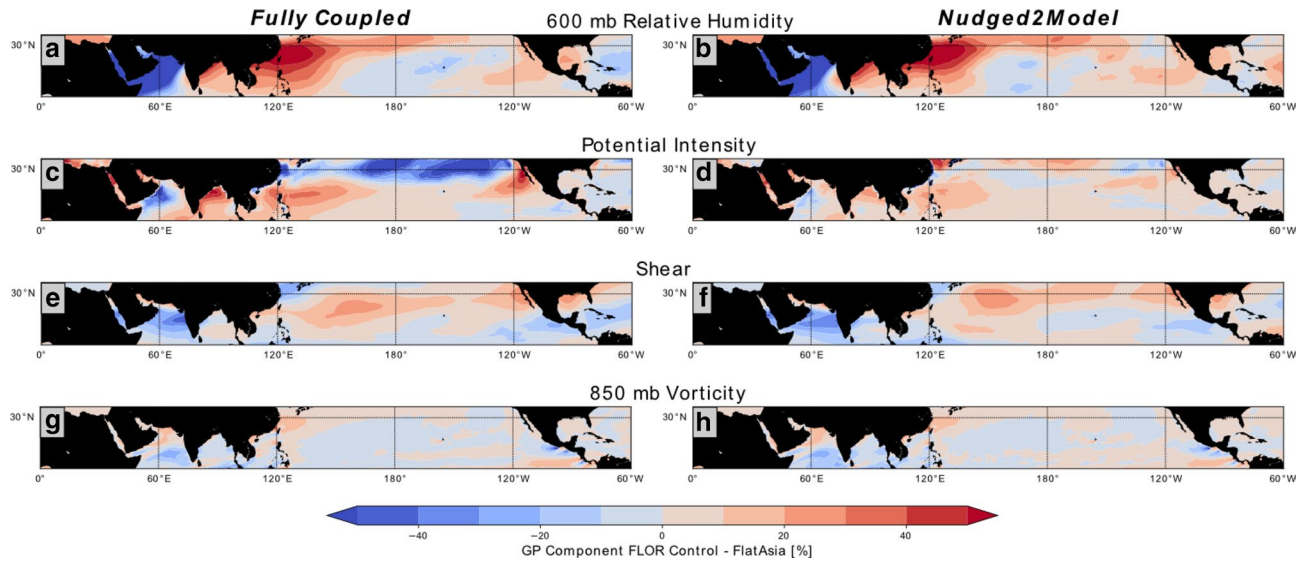


**Fig. 16** TC GP component changes due to Asian orography. Shown are changes in components for 600 mb relative humidity (**a**, **b**), potential intensity (**c**, **d**), vertical wind shear (**e**, **f**), and 850 mb absolute vorticity (**g**, **h**), from the Fully Coupled (**a**, **c**, **e**, **g**), and Nudged2Model (**b**, **d**, **f**, **h**) FLOR simulations. Each plot represents % change

of the relevant component in Eq. (3) including the factors (e.g., the wind shear term is differences in  $(1 + 0.1V_{shear})^{-2}$  so positive implies a positive contribution to GP). Note that the colorbar of this figure spans a shorter range than that of Fig. 15

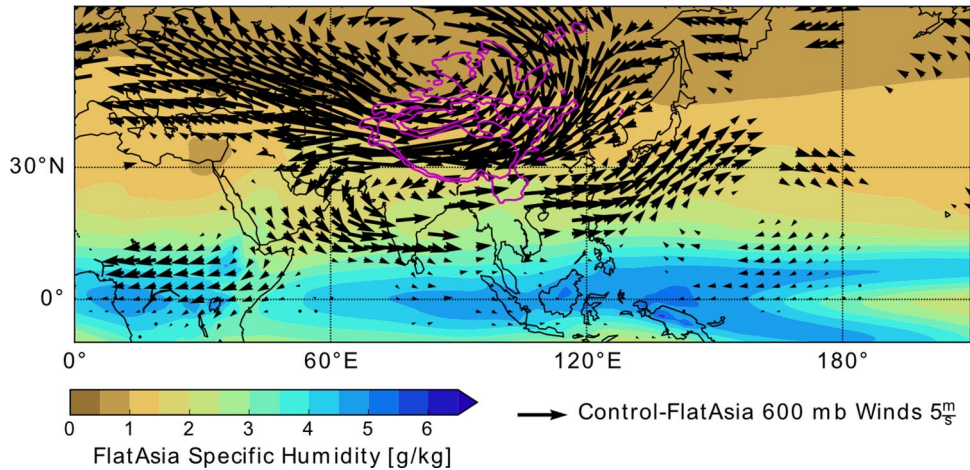


**Fig. 17** Annual mean wind changes induced by the Asian mountains overlaying mean specific humidity. Control - FlatAsia change data is from the Nudged2Model FLOR runs, and specific humidity is from the FLOR Nudged2Model FlatAsia run. Anomalies are only shown where statistically significant at the 95% level based on a two-sided

t test. Nudged2Model simulation data is used to highlight that these changes are directly driven by atmospheric circulation changes without SST response to the orography. However, results from the Fully Coupled runs are largely similar

## 4 Summary and discussion

In our simulations, Asian orography impacts monsoonal precipitation both directly through altering the atmospheric circulation, and indirectly through the atmosphere's impact on the ocean. This is shown by comparing the Fully Coupled and Nudged2Model simulations,

in which the mountains' low-frequency impact on SST is removed. Over the WNP, the mountains drive a dipole of SST change with warming to the south and cooling to the north, modulated by changes to the surface energy balance. This in turn increases the mountains' enhancement of WNP precipitation during monsoon onset (AMJ), and drives precipitation increase during the monsoon peak, a period when the mountains play little role in the prior

simulations of Park et al. (2012). Over the Arabian Sea, the mountains' enhancement of low-level southwesterlies drives coastal upwelling, SST cooling, and significantly enhances the drying over this region. Overall, the Asian mountains play a significantly larger role in monsoonal precipitation when atmosphere–ocean coupling is allowed, which echoes prior work on this topic.

There are some notable differences in our results regarding atmosphere–ocean coupling compared to prior work. As with a number of prior studies, we attribute cooling of the northern WNP largely to cloud changes (Kitoh 1997, 2002). However, we also find an important role for sensible heat fluxes. Regarding atmospheric circulation changes driving this northern WNP SST cooling, while prior work has discussed winter subtropical anticyclone enhancement (Kitoh 1997, 2002), we also describe summer cooling generated by an enhanced East Asian Monsoon. Over the southern WNP, we find decreases in latent heat fluxes drive warming by Asian orography, consistent with Okajima and Xie (2007); in contrast, Kitoh (2004) concluded that ocean circulation change drove southern WNP warming while the surface energy fluxes generated oppositional cooling. Finally, over the Arabian Sea we find cooling is generated by ocean circulation changes, and especially coastal upwelling. He et al. (2018) recently performed similar experiments examining effects of Tibetan Plateau heating, and found instead that horizontal oceanic transport and some surface energy balance changes drove Arabian Sea cooling. These differences in results could be due to a number of differences in our methodology compared to prior studies. We use higher resolution GFDL GCMs, while most prior studies use lower resolution GCMs from different modeling centers. We flatten just Asian orography while many prior studies flatten all across the globe. Finally, our method of distinguishing oceanic versus surface energy balance sources of SST change and decomposing the surface energy balance uses metrics from the SST nudging process not used in relevant prior work.

Our study also presents the first examination of the climatic influence of Asian orography with TC-permitting simulations. The mountains are found to have a large influence on the spatial distribution of TCs, increasing TC density up to 60% in the WNP, and eliminating most TCs in the Arabian Sea. Interestingly, while these are hotspots of the role of atmosphere–ocean coupling for precipitation, change in SSTs may enhance but does not seem to be the primary driver of the TC changes. Over the southern WNP, upward motion associated with the Asian mountains' stationary wave pattern increases mid-level relative humidity and in turn increases TC genesis. Over the Arabian Sea, a Gill-type cyclonic circulation response to the Asian mountains fluxes in dry air from the deserts to the west and north. Combined with remote subsidence also driven by the monsoon

heating, mid-level relative humidity in this region significantly decreases, in turn suppressing TC genesis. The climatology of the few Arabian Sea TCs in the present climate has maxima in June and November (Evan and Camargo 2011). We find that Asian orography suppresses TCs over this region from May to November, including preventing almost any TC occurrence in the peak monsoon season of JAS. However, the Arabian Sea TC climatology still exhibits the double peak even in the absence of Asian orography. This seems consistent with a weaker monsoon circulation still existing, and suppressing some summer TCs, in the FlatAsia experiments.

Overall, these regional TC changes provide new perspective on the drivers of the present pattern of TCs across the Asian sector. The WNP has some of the highest density of TCs across the globe, and while it might seem straightforward to attribute this high density to the high SSTs in this region, our results suggest a significant role for the relative humidity changes driven by the orographic landmass over Asia. In contrast, TCs are very sparse in the Arabian Sea, likely driven by the overall monsoon circulation but also enhanced by local relative humidity decrease from Asian mountains.

While precipitation changes over land were not the focus of this study, it is interesting to note that our simulations find a dipole of precipitation change over India due to Asian orography. Precipitation increases in northern India, especially close to the Himalayas, and decreases over southern India (Figs. 5 and 7). It seems this change may be contingent on atmosphere–ocean coupling: drying over southern India is not clear in the AM2.1 simulations (Fig. 2), southern India exhibits a large role for coupling in the precipitation response during AMJ (Fig. 7b), and the main other study documenting this effect also uses AOGCMs (Abe et al. 2013). The coupled response over the Arabian Sea causing cooling and drying likely bleeds into southern India, flowing along monsoonal southwesterlies, driving or at least enhancing the drying. Importantly, while Asian orography overall enhances the monsoon circulations over South Asia, such as the Findlater Jet, this does not translate to precipitation increases across all of South Asia. This conclusion echoes prior work showing that African mountains strengthen the cross-equatorial Somali Jet but do not increase monsoonal precipitation (Wei and Bordoni 2016; Chakraborty et al. 2002).

There are a number of limitations of this work which motivate further research. First, we only explored means but not climatic variability. While the tropical cyclone changes did not significantly alter the precipitation response to Asian orography on an annual mean or seasonal basis, it is plausible that they alter the variance and extremes of precipitation. Also, in this work we did not disentangle mechanical versus thermal influences of the orography. Two recent studies (He

et al. 2018; Wang et al. 2018) find that the thermal influence of the Tibetan Plateau on the South Asian monsoon circulation is reduced by atmosphere–ocean coupling. This presents an interesting contrast with our work and other studies finding enhancement of Asian orography’s precipitation change by atmosphere–ocean coupling. In light of these results, we hypothesize that it is the mechanical influence of the orography that is most enhanced by related SST changes. Finally, we only experimented with one set of flattened topographic boundary conditions. Our results should not necessarily be interpreted as primarily due to the Tibetan Plateau, as particular orographic sections such as the Mongolian Plateau and the Himalayas have an outsized impact on the winter stationary wave and the monsoon circulation respectively (White et al. 2017; Boos and Kuang 2010). Beyond studying influence of subsections of Asian orography, it would be interesting to employ the framework used in this study to explore the impact of topography already theorized or observed to be of key importance for TCs, such as the Papagayo and Tehuantepec gaps in Central America (Steenburgh et al. 1998; Zehnder et al. 1999). We have work exploring this latter question already underway.

**Acknowledgements** JWB and GAV were funded by the NOAA Climate Program Office, and JWB was also funded by a National Science Foundation Graduate Research Fellowship (DGE 1148900). Hiroyuki Murakami, Tom Delworth, Isaac Held, Chris Milly, Bill Boos, and Kerry Emanuel provided useful feedback at various stages of the project, and Seth Underwood, William Cooke, and Sergey Malyshev provided critical technical support. Two anonymous reviewers also provided thoughtful feedback which greatly improved this work. The AM2.1 simulation data was supplied by Ho-Hsuan Wei. The calculation of tropical cyclone genesis potential was significantly aided by scripts provided by Hiroyuki Murakami, for which the fortran subroutine made available online by Kerry Emanuel was used (see <https://emanuel.mit.edu/products>). We acknowledge the World Climate Research Programme’s Working Group on Coupled Modelling, which is responsible for CMIP, and we thank the participating climate modeling groups for producing and making available their model output. For CMIP the U.S. Department of Energy’s Program for Climate Model Diagnosis and Intercomparison provides coordinating support and led development of software infrastructure in partnership with the Global Organization for Earth System Science Portals.

## References

- Abe M, Kitoh A, Yasunari T (2003) An evolution of the Asian summer monsoon associated with mountain upliftsimulation with the MRI atmosphere–ocean coupled GCM. *J Meteorol Soc Jpn Ser II* 81(5):909–933
- Abe M, Yasunari T, Kitoh A (2004) Effects of large-scale orography on the coupled atmosphere–ocean system in the tropical Indian and Pacific Oceans in boreal summer. *J Meteorol Soc Jpn Ser II* 82(2):745–759
- Abe M, Yasunari T, Kitoh A (2005) Sensitivity of the central Asian climate to uplift of the Tibetan Plateau in the coupled climate model (MRI-CGCM1). *Island Arc* 14(4):378–388. <https://doi.org/10.1111/j.1440-1738.2005.00493.x>
- Abe M, Hori M, Yasunari T, Kitoh A (2013) Effects of the Tibetan Plateau on the onsetof the summer monsoon in South Asia: the role of the air-sea interaction. *J Geophys Res Atmosph* 118(4):1760–1776. <https://doi.org/10.1002/jgrd.50210>
- Adler RF, Huffman GJ, Chang A, Ferraro R, Xie PP, Janowiak J, Rudolf B, Schneider U, Curtis S, Bolvin D (2003) The version-2 global precipitation climatology project (GPCP) monthly precipitation analysis (1979–present). *J Hydrometeorol* 4(6):1147–1167
- Baldwin J, Vecchi G (2016) Influence of the Tian Shan on Arid Extratropical Asia. *J Clim* 29(16):5741–5762. <https://doi.org/10.1175/JCLI-D-15-0490.1>
- Barsugli JJ, Battisti DS (1998) The basic effects of atmosphere–ocean thermal coupling on midlatitude variability. *J Atmos Sci* 55(4):477–493. [https://doi.org/10.1175/1520-0469\(1998\)055<0477:TBEAO>2.0.CO;2](https://doi.org/10.1175/1520-0469(1998)055<0477:TBEAO>2.0.CO;2)
- Boos WR, Hurley JV (2013) Thermodynamic bias in the multimodel mean boreal summer monsoon. *J Clim* 26(7):2279–2287. <https://doi.org/10.1175/JCLI-D-12-00493.1>
- Boos WR, Kuang Z (2010) Dominant control of the South Asian monsoon by orographic insulation versus plateau heating. *Nature* 463(7278):218–222
- Boos WR, Kuang Z (2013) Sensitivity of the South Asian monsoon to elevated and non-elevated heating. *Sci Rep*. <https://doi.org/10.1038/srep01192>
- Bordoni S, Schneider T (2008) Monsoons as eddy-mediated regime transitions of the tropical overturning circulation. *Nat Geosci* 1(8):515–519. <https://doi.org/10.1038/ngeo248>
- Broccoli AJ, Manabe S (1997) Mountains and midlatitude aridity. In : Tectonic uplift and climate change pp 89–121
- Camargo SJ, Emanuel KA, Sobel AH (2007) Use of a genesis potential index to diagnose ENSO effects on tropical cyclone genesis. *J Clim* 20(19):4819–4834. <https://doi.org/10.1175/JCLI4282.1>
- Chakraborty A, Nanjundiah RS, Srinivasan J (2002) Role of Asian and African orography in Indian summer monsoon. *Geophys Res Lett* 29(20):50–51
- Chen J, Bordoni S (2014) Orographic effects of the Tibetan Plateau on the East Asian summer monsoon: an energetic perspective. *J Clim* 27(8):3052–3072
- Chiang JCH, Fung IY, Wu CH, Cai Y, Edman JP, Liu Y, Day JA, Bhattacharya T, Mondal Y, Labrousse CA (2015) Role of seasonal transitions and westerly jets in East Asian paleoclimate. *Quat Sci Rev* 108:111–129. <https://doi.org/10.1016/j.quascirev.2014.11.009>
- Clement AC, Burgman R, Norris JR (2009) Observational and model evidence for positive low-level cloud feedback. *Science* 325(5939):460–464. <https://doi.org/10.1126/science.1171255>
- Cohen NY, Boos WR (2017) The influence of orographic Rossby and gravity waves on rainfall. *Q J R Meteorol Soc* 143(703):845–851. <https://doi.org/10.1002/qj.2969>
- Delworth TL, Rosati A, Anderson W, Adcroft AJ, Balaji V, Benson R, Dixon K, Griffies SM, Lee HC, Pacanowski RC (2012) Simulated climate and climate change in the GFDL CM2. *J Clim* 5 High-resolution Coupled Clim Model 25(8):2755–2781
- Edwards M (1988) Data announcement 88-MGG-02: digital relief of the surface of the earth. National Oceanic and Atmospheric Administration, Boulder
- Evan AT, Camargo SJ (2011) A climatology of Arabian Sea cyclonic storms. *J Clim* 24(1):140–158
- Fallah B, Cubasch U, Prummel K, Sodoudi S (2015) A numerical model study on the behaviour of Asian summer monsoon and AMOC due to orographic forcing of Tibetan Plateau. *Clim Dyn*. <https://doi.org/10.1007/s00382-015-2914-5>
- Gadgil S, Kumar KR (2006) The Asian monsoon agriculture and economy. In: The Asian monsoon, Springer Praxis Books. Springer, Berlin, pp 651–683. [https://doi.org/10.1007/3-540-37722-0\\_18](https://doi.org/10.1007/3-540-37722-0_18)

- Gill AE (1980) Some simple solutions for heat-induced tropical circulation. *Q J R Meteorol Soc* 106(449):447–462. <https://doi.org/10.1002/qj.49710644905>
- Hahn DG, Manabe S (1975) The role of mountains in the south Asian monsoon circulation. *J Atmos Sci* 32(8):1515–1541
- Harris LM, Lin SJ, Tu C (2016) High-resolution climate simulations using GFDL HiRAM with a stretched global grid. *J Clim* 29(11):4293–4314
- He B, Liu Y, Wu G, Wang Z, Bao Q (2018) The role of air-sea interactions in regulating the thermal effect of the Tibetan-Iranian Plateau on the Asian summer monsoon. *Clim Dyn.* <https://doi.org/10.1007/s00382-018-4377-y>
- Hoskins B, Wang B (2006) Large-scale atmospheric dynamics. The Asian monsoon. Springer, Berlin, pp 357–415
- Hoskins BJ, Karoly DJ (1981) The steady linear response of a spherical atmosphere to thermal and orographic forcing. *J Atmos Sci* 38(6):1179–1196
- Huffman GJ, Bolvin DT, Nelkin EJ, Wolff DB, Adler RF, Gu G, Hong Y, Bowman KP, Stocker EF (2007) The TRMM multisatellite precipitation analysis (TMPA): quasi-global, multiyear, combined-sensor precipitation estimates at fine scales. *J Hydrometeorol* 8(1):38–55. <https://doi.org/10.1175/JHM560.1>
- Jia L, Yang X, Vecchi GA, Gudgel RG, Delworth TL, Rosati A, Stern WF, Wittenberg AT, Krishnamurthy L, Zhang S, Msadek R, Kapnick S, Underwood S, Zeng F, Anderson WG, Balaji V, Dixon K (2014) Improved seasonal prediction of temperature and precipitation over land in a high-resolution GFDL climate model. *J Clim* 28(5):2044–2062. <https://doi.org/10.1175/JCLI-D-14-00112.1>
- Jiang H, Zipser EJ (2010) Contribution of tropical cyclones to the global precipitation from eight seasons of TRMM data: regional, seasonal, and interannual variations. *J Clim* 23(6):1526–1543
- Kapnick SB, Delworth TL, Ashfaq M, Malyshev S, Milly PC (2014) Snowfall less sensitive to warming in Karakoram than in Himalayas due to a unique seasonal cycle. *Nat Geosci* 7(11):834
- Khouakhi A, Villarini G, Vecchi GA (2016) Contribution of tropical cyclones to rainfall at the global scale. *J Clim* 30(1):359–372. <https://doi.org/10.1175/JCLI-D-16-0298.1>
- Kitoh A (1997) Mountain uplift and surface temperature changes. *Geophys Res Lett* 24(2):185–188
- Kitoh A (2002) Effects of large-scale mountains on surface climate – coupled ocean-atmosphere general circulation model study. *J Meteorol Soc Jpn Ser II* 80(5):1165–1181
- Kitoh A (2004) Effects of mountain uplift on East Asian summer climate investigated by a coupled atmosphere-ocean GCM. *J Clim* 17(4):783–802. [https://doi.org/10.1175/1520-0442\(2004\)017<0783:EOMUOE>2.0.CO;2](https://doi.org/10.1175/1520-0442(2004)017<0783:EOMUOE>2.0.CO;2)
- Kitoh A (2007) ENSO modulation by mountain uplift. *Clim Dyn* 28(7–8):781–796. <https://doi.org/10.1007/s00382-006-0209-6>
- Kitoh A, Motoi T, Arakawa O (2010) Climate modelling study on mountain uplift and Asian monsoon evolution. *Geol Soc Lond Special Publ Spec* 342(1):293–301. <https://doi.org/10.1144/SP342.17>
- Klein SA, Hartmann DL (1993) The seasonal cycle of low stratiform clouds. *J Clim* 6(8):1587–1606
- Koseki S, Watanabe M, Kimoto M (2008) Role of the midlatitude air-sea interaction in orographically forced climate. *J Meteorol Soc Jpn Ser II* 86(2):335–351. <https://doi.org/10.2151/jmsj.86.335>
- Krishnamurthy L, Vecchi GA, Msadek R, Murakami H, Wittenberg A, Zeng F (2016) Impact of strong ENSO on regional tropical cyclone activity in a high-resolution climate model in the North Pacific and North Atlantic Oceans. *J Clim* 29(7):2375–2394
- Krishnamurthy L, Vecchi GA, Yang X, van der Wiel K, Balaji V, Kapnick SB, Jia L, Zeng F, Paffendorf K, Underwood S (2018) Causes and probability of occurrence of extreme precipitation events like Chennai 2015. *J Clim.* <https://doi.org/10.1175/JCLI-D-17-0302.1>
- Kutzbach JE, Prell WL, Ruddiman WF (1993) Sensitivity of Eurasian climate to surface uplift of the Tibetan Plateau. *J Geol* 101(2):177–190
- Lee JY, Wang B, Seo KH, Ha KJ, Kitoh A, Liu J (2015) Effects of mountain uplift on global monsoon precipitation. *Asia-Pac J Atmos Sci* 51(3):275–290
- Lee SS, Lee JY, Ha KJ, Wang B, Kitoh A, Kajikawa Y, Abe M (2013) Role of the Tibetan plateau on the annual variation of mean atmospheric circulation and storm track activity. *J Clim* 26(14):5270–5286
- Leetmaa A (1972) The response of the Somali Current to the southwest monsoon of 1970. *Deep Sea Res Oceanogr Abstr* 19(4):319–325. [https://doi.org/10.1016/0011-7471\(72\)90025-3](https://doi.org/10.1016/0011-7471(72)90025-3)
- Liu X, Yin ZY (2002) Sensitivity of East Asian monsoon climate to the uplift of the Tibetan Plateau. *Palaeogeogr Palaeoclimatol Palaeoecol* 183(34):223–245. [https://doi.org/10.1016/S0031-0182\(01\)00488-6](https://doi.org/10.1016/S0031-0182(01)00488-6)
- Ma D, Boos W, Kuang Z (2014) Effects of orography and surface heat fluxes on the South Asian summer monsoon. *J Clim* 27(17):6647–6659. <https://doi.org/10.1175/JCLI-D-14-00138.1>
- Milly PC, Malyshev SL, Shevliakova E, Dunne KA, Findell KL, Gleeson T, Liang Z, Phillipps P, Stouffer RJ, Swenson S (2014) An enhanced model of land water and energy for global hydrologic and earth-system studies. *J Hydrometeorol* 15(5):1739–1761
- Molnar P, Boos WR, Battisti DS (2010) Orographic controls on climate and paleoclimate of Asia: thermal and mechanical roles for the Tibetan Plateau. *Ann Rev Earth Planet Sci* 38(1):77
- Murakami H, Vecchi GA, Underwood S, Delworth TL, Wittenberg AT, Anderson WG, Chen JH, Gudgel RG, Harris LM, Lin SJ, Zeng F (2015) Simulation and prediction of category 4 and 5 hurricanes in the high-resolution GFDL HiFLOR coupled climate model. *J Clim* 28(23):9058–9079. <https://doi.org/10.1175/JCLI-D-15-0216.1>
- Norris JR, Leovy CB (1994) Interannual variability in stratiform cloudiness and sea surface temperature. *J Clim* 7(12):1915–1925
- Okajima H, Xie SP (2007) Orographic effects on the northwestern Pacific monsoon: role of air-sea interaction. *Geophys Res Lett* 34(21):L21708. <https://doi.org/10.1029/2007GL032206>
- Park HS, Chiang JCH, Son SW (2010) The role of the central Asian mountains on the midwinter suppression of north Pacific storminess. *J Atmos Sci* 67(11):3706–3720. <https://doi.org/10.1175/2010JAS3349.1>
- Park HS, Chiang JC, Bordoni S (2012) The mechanical impact of the Tibetan Plateau on the seasonal evolution of the South Asian monsoon. *J Clim* 25(7):2394–2407
- Prell WL, Kutzbach JE (1992) Sensitivity of the Indian monsoon to forcing parameters and implications for its evolution. *Nature* 360(6405):647
- Rayner NA, Parker DE, Horton EB, Folland CK, Alexander LV, Rowell DP, Kent EC, Kaplan A (2003) Global analyses of sea surface temperature, sea ice, and night marine air temperature since the late nineteenth century. *J Geophys Res Atmos* 108(D14):1–29
- Reynolds RW, Rayner NA, Smith TM, Stokes DC, Wang W (2002) An improved in situ and satellite SST analysis for climate. *J Clim* 15(13):1609–1625
- Rienecker MM, Suarez MJ, Gelaro R, Todling R, Bacmeister J, Liu E, Bosilovich MG, Schubert SD, Takacs L, Kim GK (2011) MERRA: NASA's modern-era retrospective analysis for research and applications. *J Clim* 24(14):3624–3648
- Rind D, Russell G, Ruddiman WF (1997) The effects of uplift on ocean-atmosphere circulation. In: Ruddiman WF (ed) *Tectonic uplift and climate change*, Springer, Boston, pp 123–147. [https://doi.org/10.1007/978-1-4615-5935-1\\_6](https://doi.org/10.1007/978-1-4615-5935-1_6)
- Rodwell MJ, Hoskins BJ (1996) Monsoons and the dynamics of deserts. *Q J R Meteorol Soc* 122(534):1385–1404

- Sampe T, Xie SP (2010) Large-scale dynamics of the Meiyu-Baiu Rainband: environmental forcing by the westerly jet. *J Clim* 23(1):113–134
- Shi X, Wang Y, Xu X (2008) Effect of mesoscale topography over the Tibetan Plateau on summer precipitation in China: a regional model study. *Geophys Res Lett* 35(19):L19707. <https://doi.org/10.1029/2008GL034740>
- Shi Z, Liu X, Liu Y, Sha Y, Xu T (2014) Impact of Mongolian Plateau versus Tibetan Plateau on the westerly jet over North Pacific Ocean. *Clim Dyn* 44(11–12):3067–3076. <https://doi.org/10.1007/s00382-014-2217-2>
- Simpson IR, Seager R, Shaw TA, Ting M (2015) Mediterranean summer Climate and the importance of Middle East topography. *J Clim* 28(5):1977–1996
- Steenburgh WJ, Schultz DM, Colle BA (1998) The structure and evolution of gap outflow over the gulf of Tehuantepec Mexico. *Mon Weather Rev* 126(10):2673–2691. [https://doi.org/10.1175/1520-0493\(1998\)126<2673:TSAEOG>2.0.CO;2](https://doi.org/10.1175/1520-0493(1998)126<2673:TSAEOG>2.0.CO;2)
- Stocker TF (2014) Climate change 2013: the physical science basis: Working Group I contribution to the fifth assessment report of the Intergovernmental Panel on climate change. Cambridge University Press, Cambridge
- Tang H, Micheels A, Eronen JT, Ahrens B, Fortelius M (2012) Asynchronous responses of East Asian and Indian summer monsoons to mountain uplift shown by regional climate modelling experiments. *Clim Dyn* 40(5–6):1531–1549. <https://doi.org/10.1007/s00382-012-1603-x>
- Taylor KE, Stouffer RJ, Meehl GA (2012) An overview of CMIP5 and the experiment design. *Bull Am Meteorol Soc* 93(4):485–498
- Vecchi GA, Delworth T, Gudgel R, Kapnick S, Rosati A, Wittenberg AT, Zeng F, Anderson W, Balaji V, Dixon K (2014) On the seasonal forecasting of regional tropical cyclone activity. *J Clim* 27(21):7994–8016
- Wang Z, Duan A, Yang S (2018) Potential regulation on the climatic effect of Tibetan Plateau heating by tropical airsea coupling in regional models. *Clim Dyn*. <https://doi.org/10.1007/s00382-018-4218-z>
- Wei HH, Bordoni S (2016) On the role of the African topography in the South Asian monsoon. *J Atmos Sci* 73(8):3197–3212. <https://doi.org/10.1175/JAS-D-15-0182.1>
- White RH, Battisti DS, Roe GH (2017) Mongolian mountains matter most: impacts of the latitude and height of Asian orography on Pacific wintertime atmospheric circulation. *J Clim* 30(11):4065–4082
- van der Wiel K, Kapnick SB, Vecchi GA, Cooke WF, Delworth TL, Jia L, Murakami H, Underwood S, Zeng F (2016) The resolution dependence of contiguous U.S. precipitation extremes in response to CO<sub>2</sub> forcing. *J Clim* 29(22):7991–8012
- Wu G, Liu Y, He B, Bao Q, Duan A, Jin FF (2012) Thermal controls on the Asian summer monsoon. *Sci Rep*. <https://doi.org/10.1038/srep00404>
- Xie P, Arkin PA (1997) Global precipitation: a 17-year monthly analysis based on gauge observations, satellite estimates, and numerical model outputs. *Bull Am Meteorol Soc* 78(11):2539–2558
- Ye PDDZ, Wu GX (1998) The role of the heat source of the Tibetan Plateau in the general circulation. *Meteorol Atmos Phys* 67(1–4):181–198. <https://doi.org/10.1007/BF01277509>
- Zehnder JA, Powell DM, Ropp DL (1999) The interaction of east–east waves, orography, and the intertropical convergence zone in the genesis of eastern Pacific tropical cyclones. *Mon Weather Rev* 127(7):1566–1585. [https://doi.org/10.1175/1520-0493\(1999\)127<1566:TIOEWO>2.0.CO;2](https://doi.org/10.1175/1520-0493(1999)127<1566:TIOEWO>2.0.CO;2)
- Zhang W, Vecchi GA, Murakami H, Delworth T, Wittenberg AT, Rosati A, Underwood S, Anderson W, Harris L, Gudgel R, Lin SJ, Villarini G, Chen JH (2015) Improved simulation of tropical cyclone responses to ENSO in the western north Pacific in the high-resolution GFDL HiFLOR coupled climate model. *J Clim* 29(4):1391–1415. <https://doi.org/10.1175/JCLI-D-15-0475.1>
- Zhang W, Vecchi GA, Murakami H, Villarini G, Jia L (2016) The pacific meridional mode and the occurrence of tropical cyclones in the western north Pacific. *J Clim* 29(1):381–398

**Publisher's Note** Springer Nature remains neutral with regard to jurisdictional claims in published maps and institutional affiliations.